Optics of Marine Particles

Lecture 1

Dariusz Stramski

Scripps Institution of Oceanography
University of California San Diego
Email: dstramski@ucsd.edu

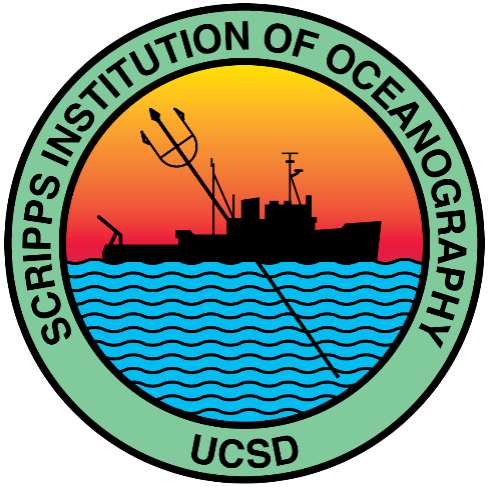

IOCCG Summer Lecture Series
22 July - 2 August 2014, Villefranche-sur-Mer, France

What is ocean optics?

In principle it sounds straightforward, but in reality it's not...

Seawater is a highly complex medium containing a “witch's brew” of dissolved substances and suspended particles which strongly alter its optical properties.

Microscopic plankton

Because of this, ocean optics is a strongly interdisciplinary science combining physics, biology, chemistry, geology, and atmospheric sciences.

OCEAN OPTICS RESEARCH LAB AT SIO

PARTICLE OPTICS

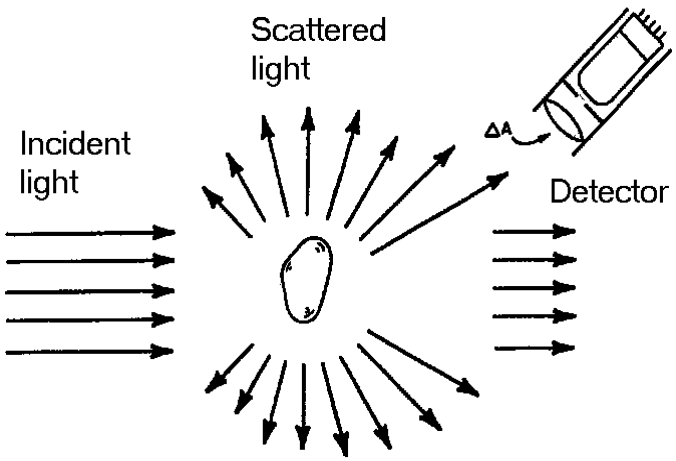

FIELD OBSERVATIONS

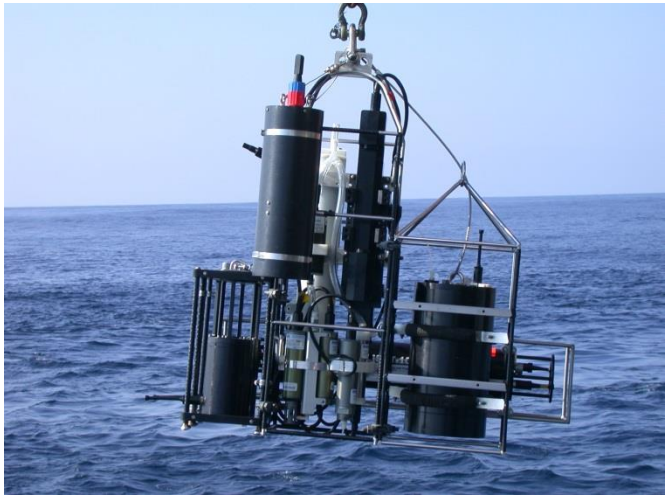

MODELING

$$\cos\theta \frac{dL(z,\xi,\lambda)}{dz} = -c(z,\lambda)L(z,\xi,\lambda)$$

$$+ \int_{\Xi} L(z,\xi',\lambda)\beta(z,\xi' \rightarrow \xi,\lambda)d\Omega(\xi')$$

$$+ S(z,\xi,\lambda)$$

REMOTE SENSING

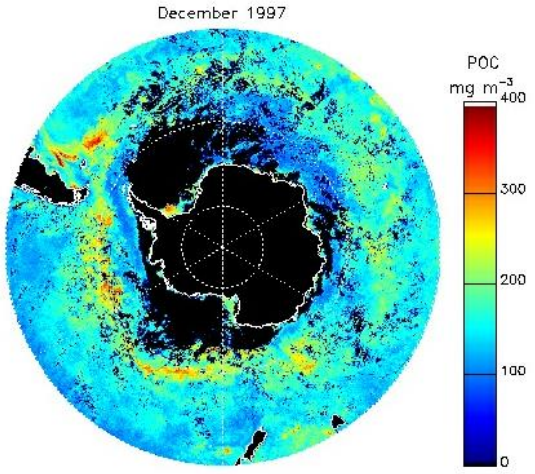

Seawater is a complex optical medium with a great variety of particle types and soluble species

- Molecular water
- Inorganic salts
- Dissolved organic matter
- Plankton microorganisms
- Organic detrital particles
- Mineral particles
- Colloidal particles
- Air bubbles

Suspended Particulate Matter

Diversity of biological and mineral particles

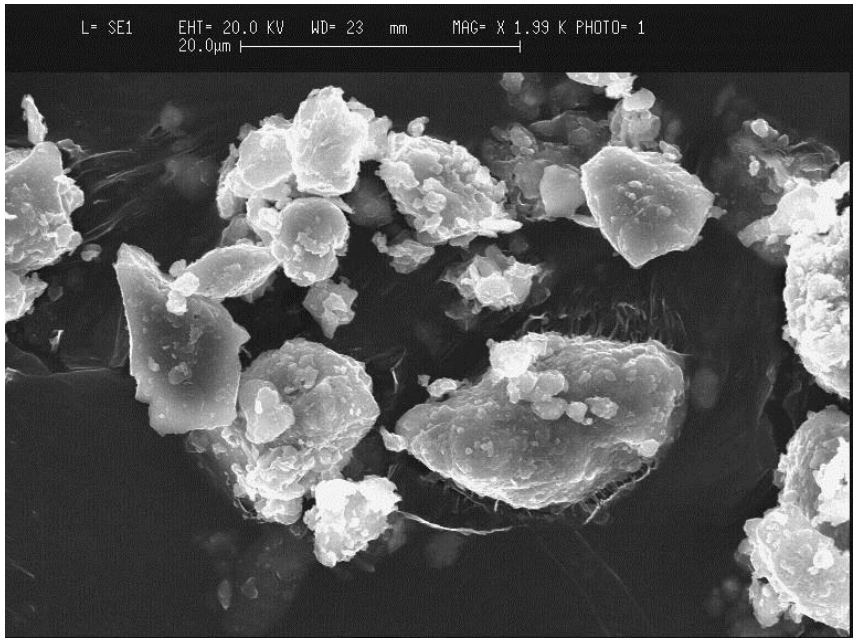

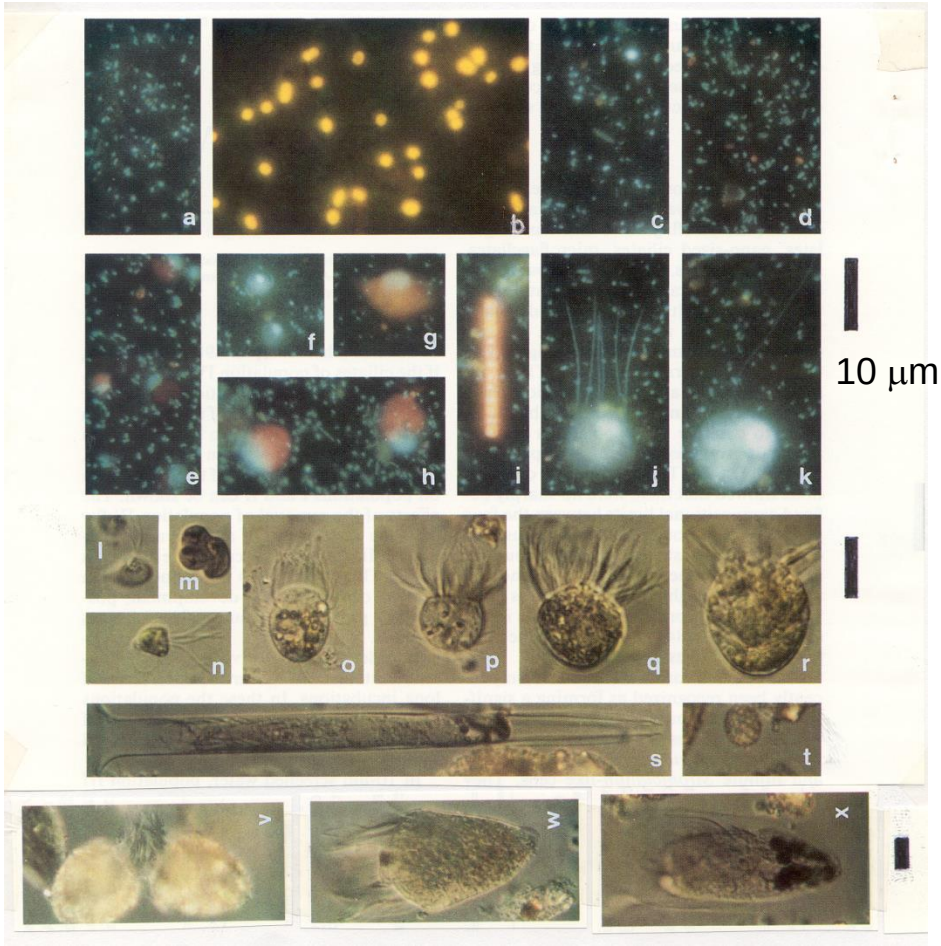

Long-term goals

- Understand the magnitudes and variability of oceanic optical properties
- Predict ocean optical properties given the types and concentration of suspended particles (*forward problem*)
- Obtain bio-optical properties and biogeochemical information from optical in situ and remote-sensing measurements (*inverse problem*)

OCEAN COLOR

$$R_{rs}(\lambda) \equiv \frac{L_w(\lambda)_{z=0^+}}{E_d(\lambda)_{z=0^+}} \propto \frac{b_b(\lambda)}{a(\lambda)}$$

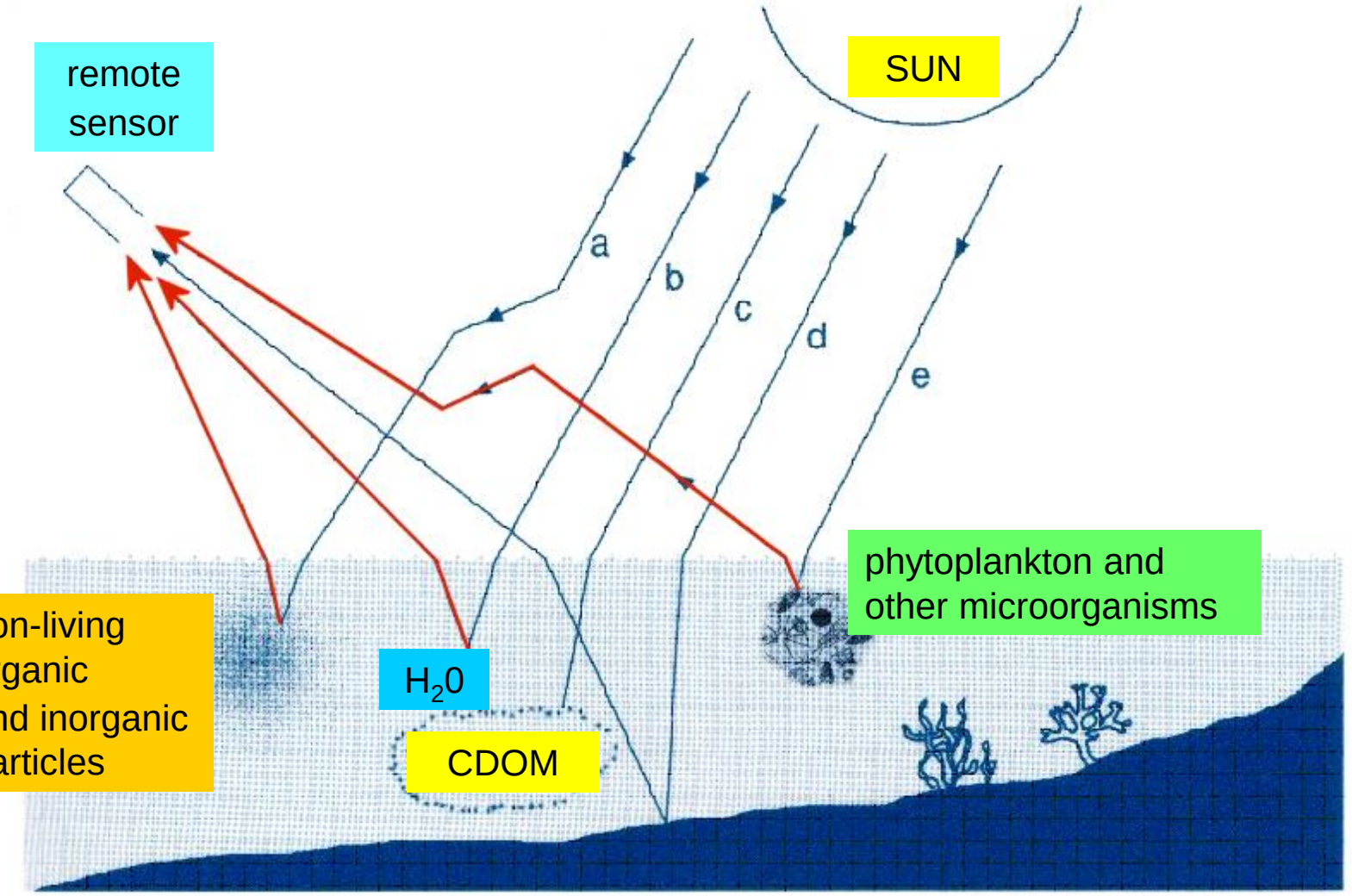

Direct problem

Dragon

?

Tracks

Inverse problem

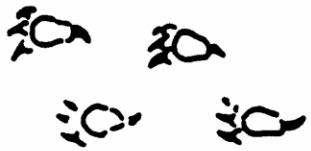

Tracks

?

Dragon

(Bohren and Huffman 1983)

Interaction of light with matter

Scattering - life of a photon

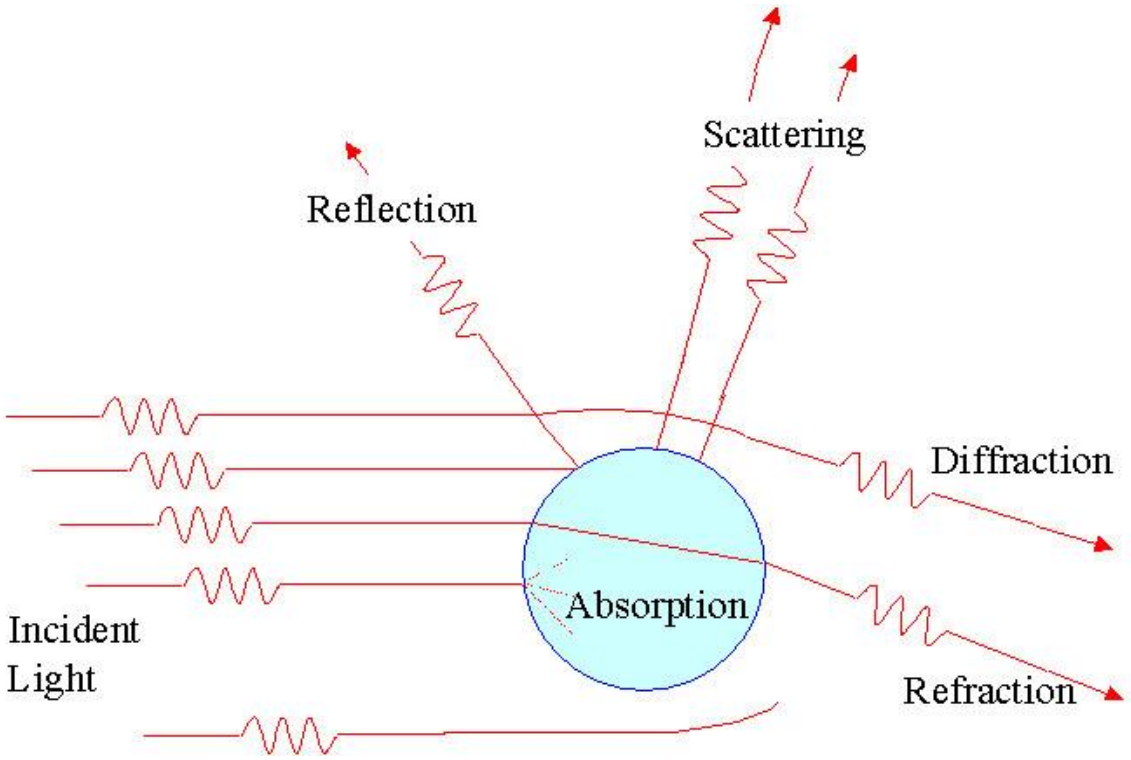

Absorption - death of a photon

“Physics should be made as simple as possible, but no simpler”

- Albert Einstein

Energy levels of molecules: Mechanism of light absorption

Electronic:
energy ~400 kJ/mol
λ ~100 – 1000 nm

Vibrational:
energy ~4 – 40 kJ/mol
λ ~1 – 20 μm

Rotational:
energy ~10^{-2} – 10^{-3} kJ/mol
λ > 20 μm

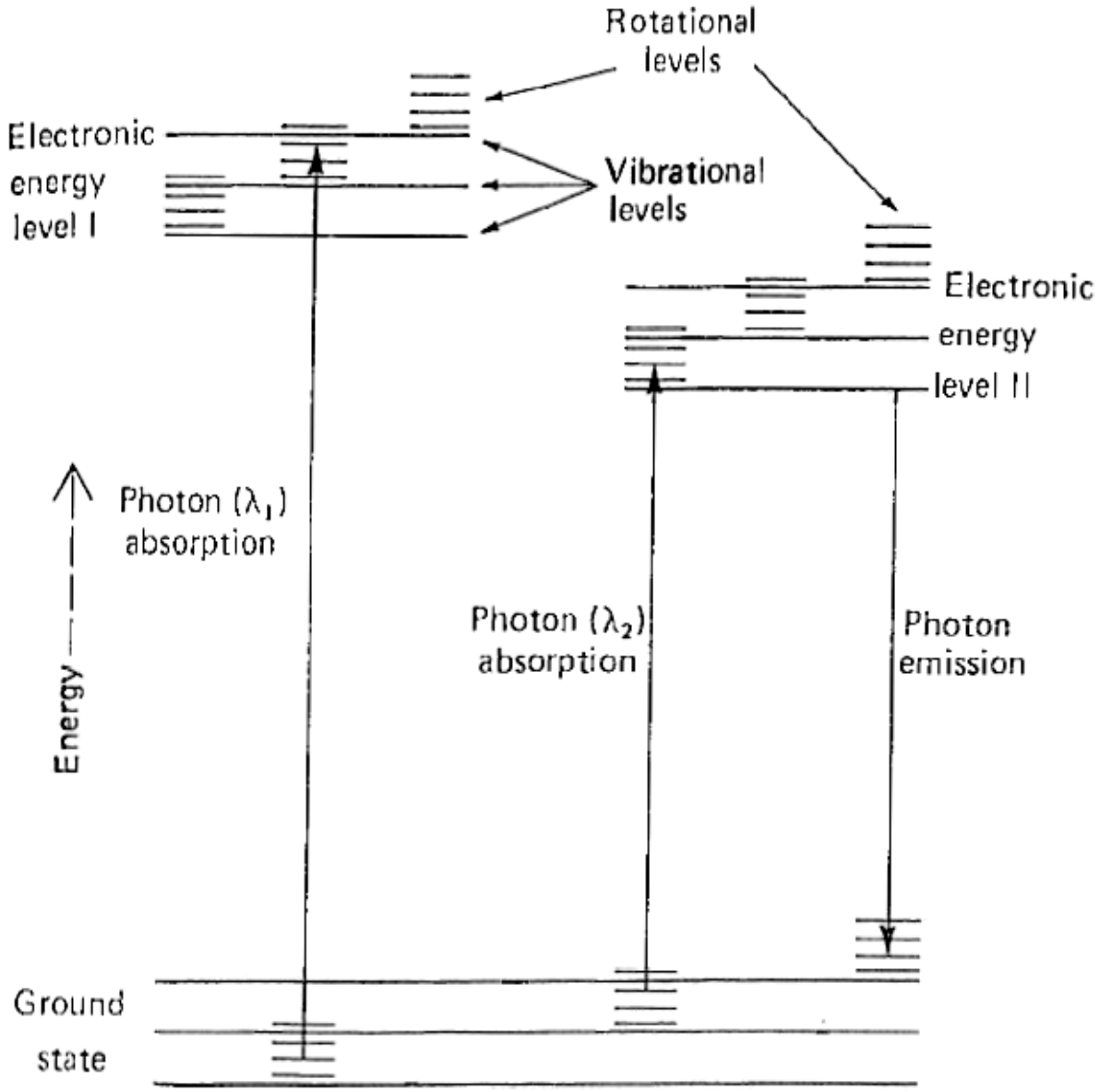

(Kirk 1994)

Absorption efficiency factor for particles

$Q_a(\lambda) = F_a(\lambda) / F_o(\lambda)$

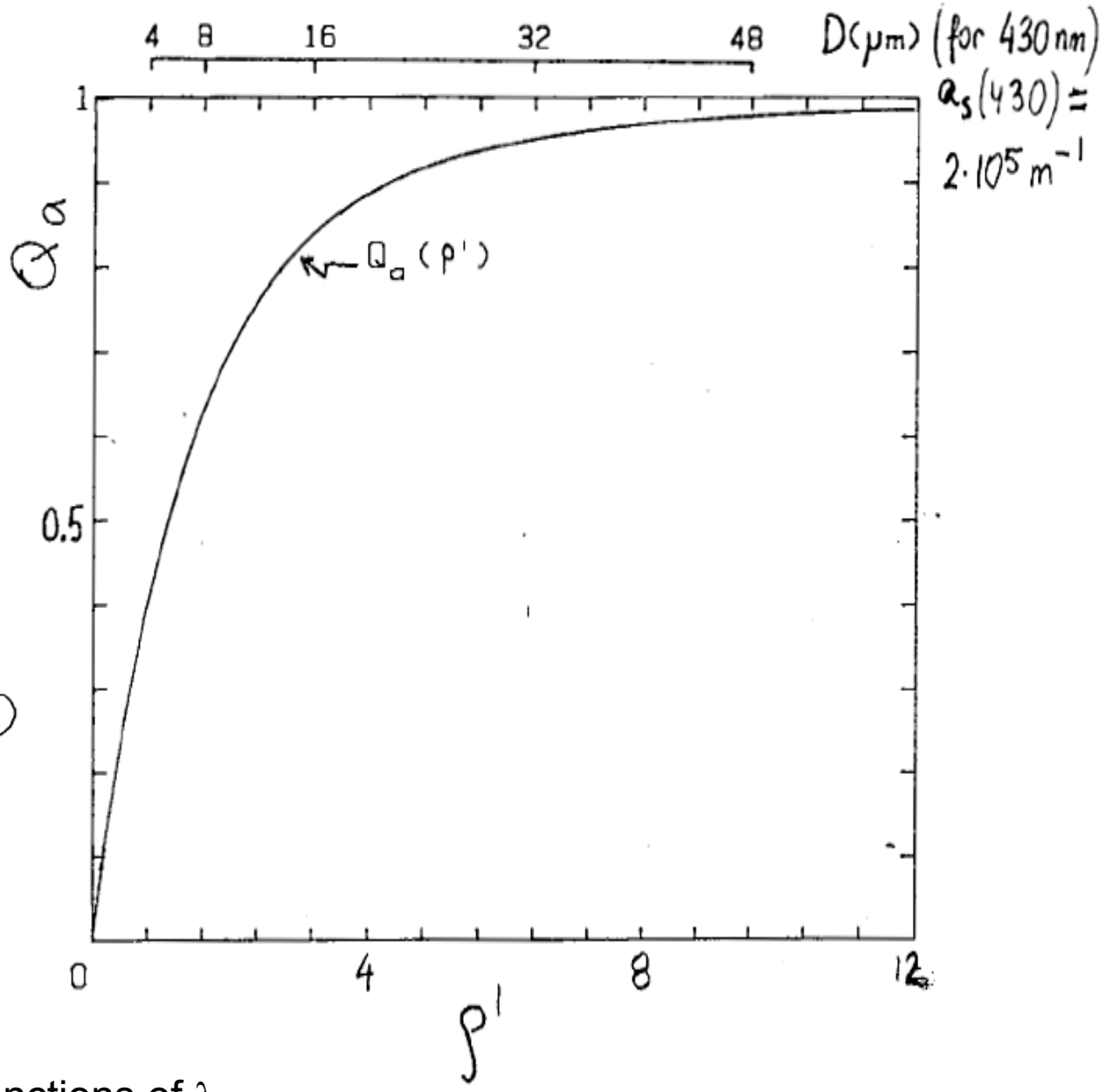

particle in water

$$\rho' = 4 \alpha n' = a_s D$$

$$\alpha = \frac{\pi \cdot D \cdot n_w}{\lambda}$$

$$n' = \frac{\lambda a_s}{4 \pi n_w}$$

Note: Q_a, a_s, and n' are functions of λ

(Morel and Bricaud 1981)

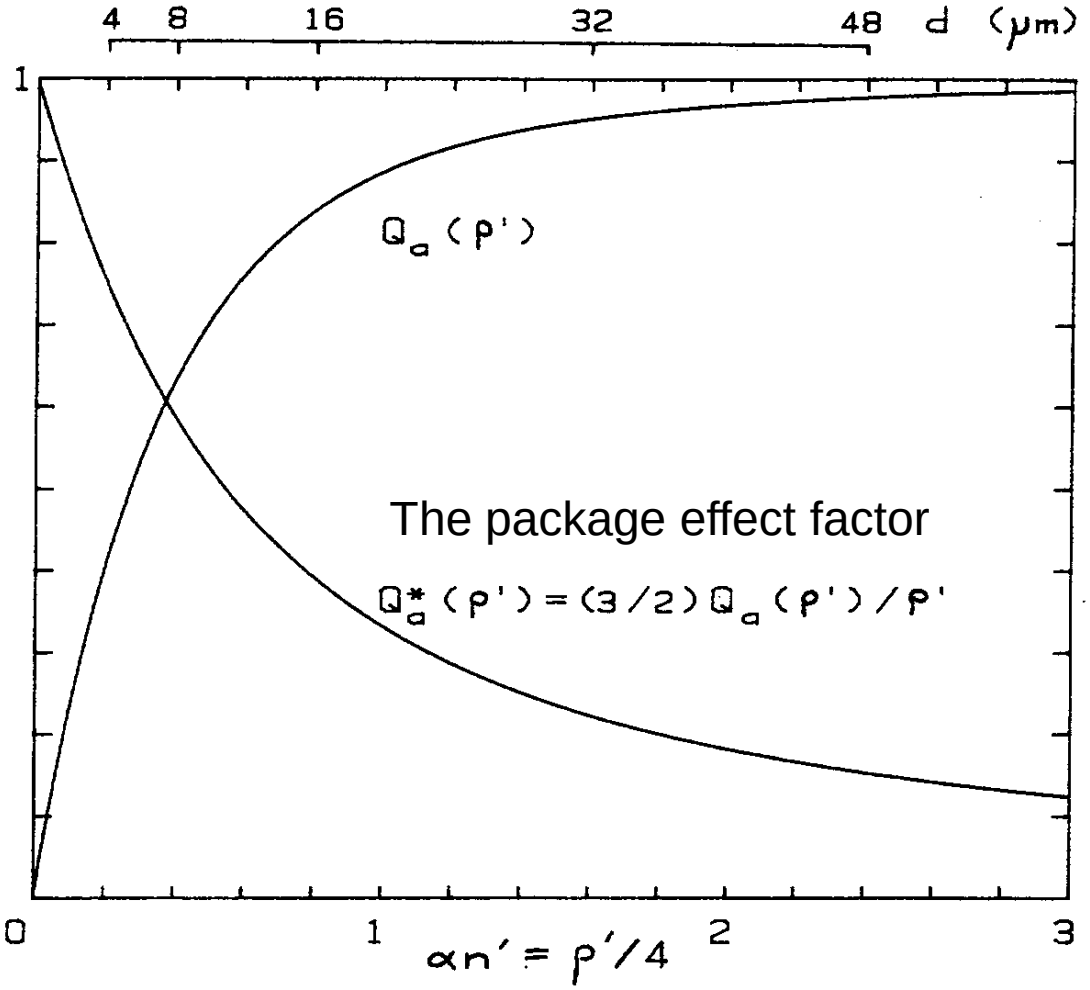

Fig. 1. Dimensionless functions Q_a and Q_a^* (equations 1 and 6) plotted vs $\alpha n'$. The corresponding scale in diameter d (μm) is obtained assuming that the absorption coefficient, a_{cm}, for the cellular material is equal to 2×10^5 m^{-1}, which is a representative mean value for many algal cells at $\lambda = 430$ nm (see text). Note that $\rho' = da_{cm} = 4\alpha n'$.

(Morel and Bricaud 1981)

Linkage between the single-particle optical properties and bulk optical properties of particle suspension

$$a = (N/V)\, Q_a\, G = (N/V)\, \sigma_a$$

a is the absorption coefficient of a collection of particles in aqueous suspension (units of m^{-1})

N/V is the number of particles per unit volume of water (units of m^{-3})

Q_a is the absorption efficiency factor (dimesionless)

G is the area of cross section of a particle (units of m^2). For spherical particles $G = (\pi/4)D^2$ where D is a diameter

σ_a ($= Q_a\, G$) is the absorption cross-section (units of m^2)

Note: a, Q_a, and σ_a are the spectral quantities (i.e., functions of light wavelength)

The package effect

$a^* = a / Chl = a / [(Chl_{cell}/V_{cell})\ (N/V) V_{cell}] = a / [Chl_i\ (N/V) V_{cell}]$

For spherical particles:

$a = (N/V)\ Q_a\ (\pi/4) D^2$ and $V_{cell} = (\pi/6) D^3$

$a^* = (3/2)\ Q_a / (Chl_i\ D) = (3/2)\ (a_s / Chl_i)\ [Q_a / (a_s\ D)] =$

$= (3/2)\ (a_s / Chl_i)\ (Q_a / \rho') = (a_s / Chl_i)\ Q^*_a = a^*_{sol}\ Q^*_a$

where $a^*_{sol} = a_s / Chl_i$

$a^* = a^*_{sol}$ if $\rho' \rightarrow 0$ and $Q^*_a = 1$

The package effect factor:

$Q^*_a = a^* / a^*_{sol} = (3/2)\ Q_a / \rho' = (3/2)\ Q_a / (a_s\ D)$

(Morel and Bricaud 1981)

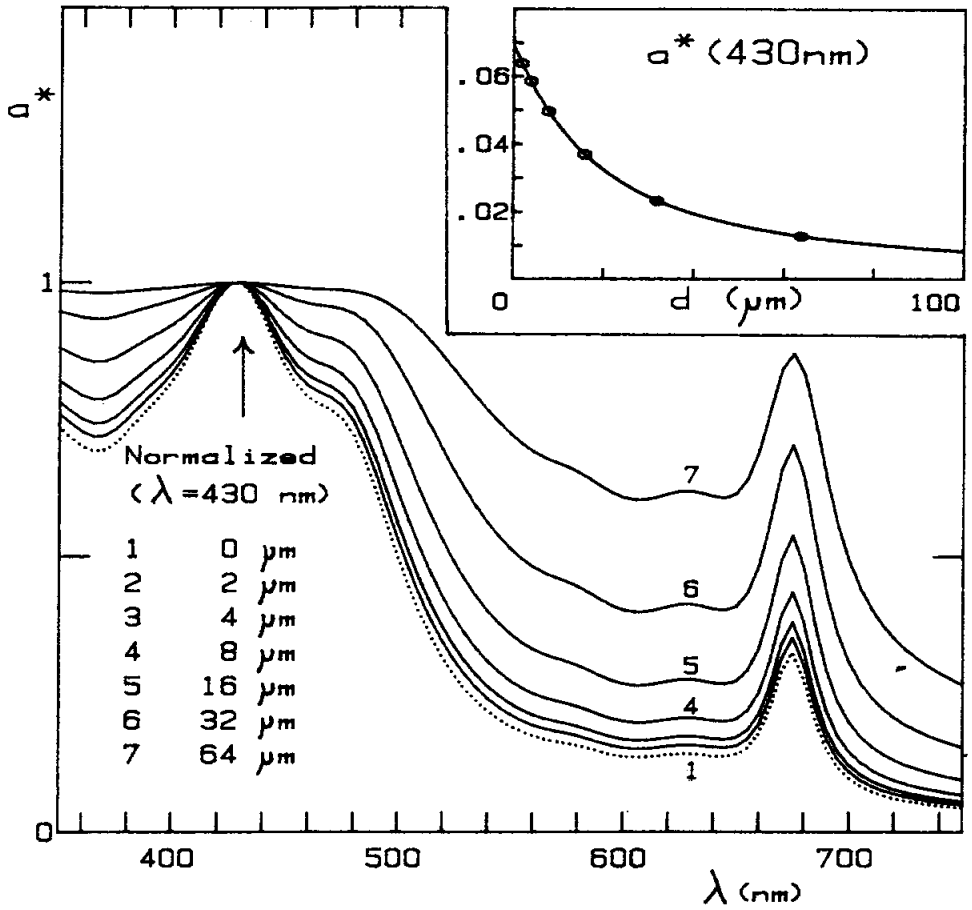

Fig. 2. Change in spectral absorption values with variable cell size (diameter, d, in μm) whereas the cell material forming the cells remains unchanged. The spectral absorption values of this material, somewhat arbitrarily adopted, are shown as the dotted curve. All curves are normalized, at $\lambda = 430$ nm, to evidence the progressive deformation. The variations with size of the specific absolute value at 430 nm (m^2 mg^{-1} Chl a) are shown in inset, under the same assumption of a constant absorption of the cell material ($a_{cm} = 2 \times 10^5$ m^{-1} at 430 nm) and with the additional assumption of a constant intracellular pigment concentration ($c_i = 2.86 \times 10^6$ mg Chl a m^{-3}).

(Morel and Bricaud 1981)

Solid lines: intact cells in cultures

Dotted lines: hypothetical aqueous solution of the material forming the cells

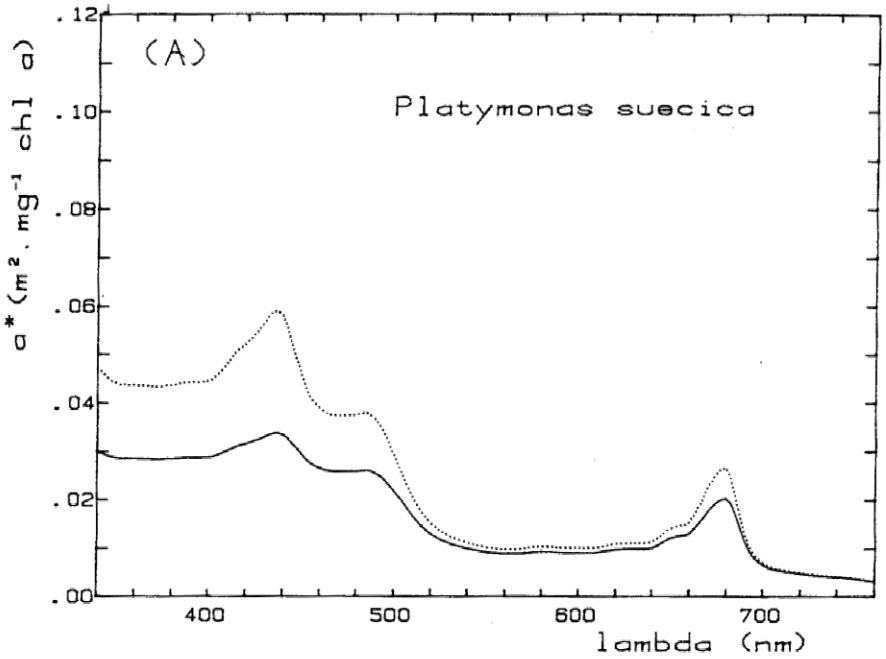

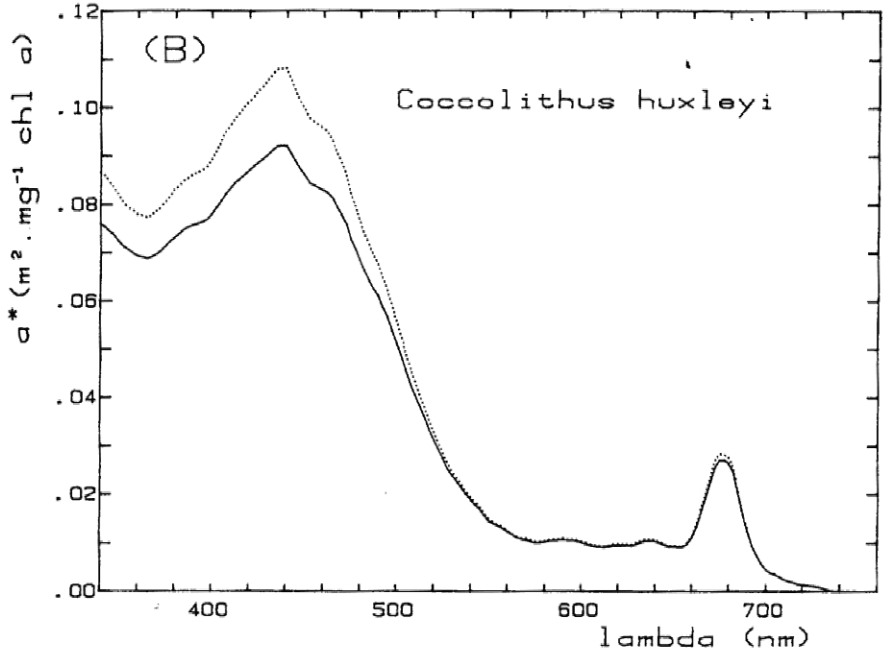

(Morel and Bricaud 1981)

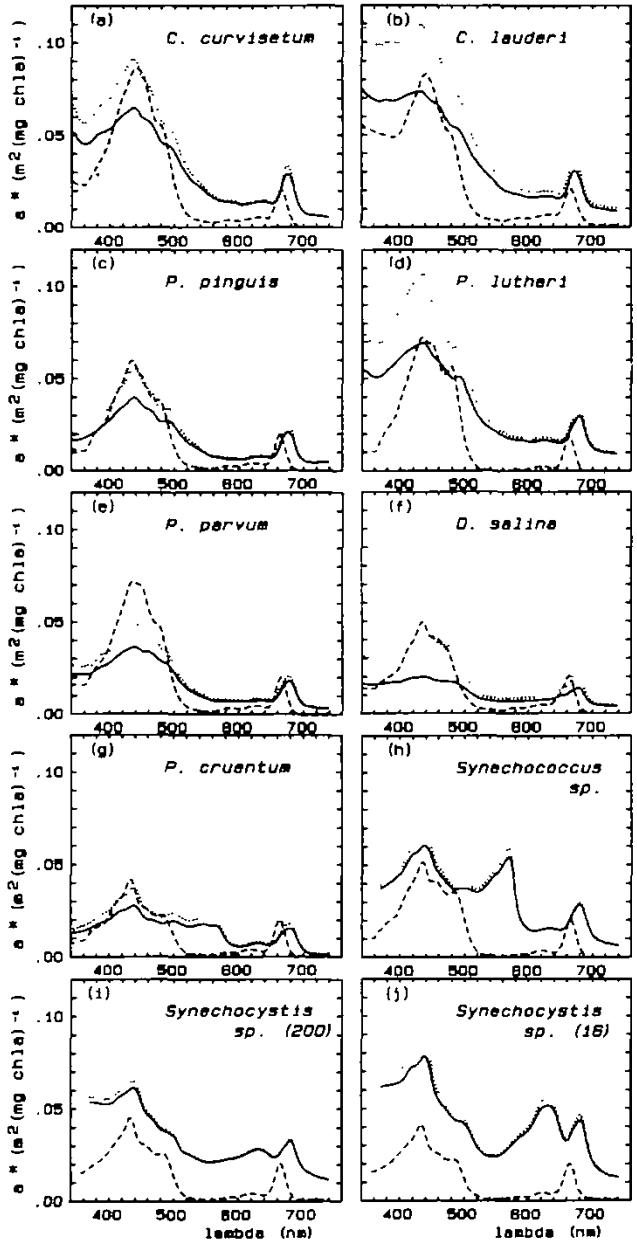

Fig. 1. Spectral values of the chl *a*-specific absorption coefficients measured for intact cells [$a^*_{sus}(\lambda)$, solid line], computed for a hypothetical aqueous solution of the cell material [$a^*_{sol}(\lambda)$, dotted line] and measured after acetone extraction [$a^*_{ext}(\lambda)$, dashed line].

(Bricaud et al. 1988)

Absorption efficiency for various phytoplankton and heterotrophic microorganisms

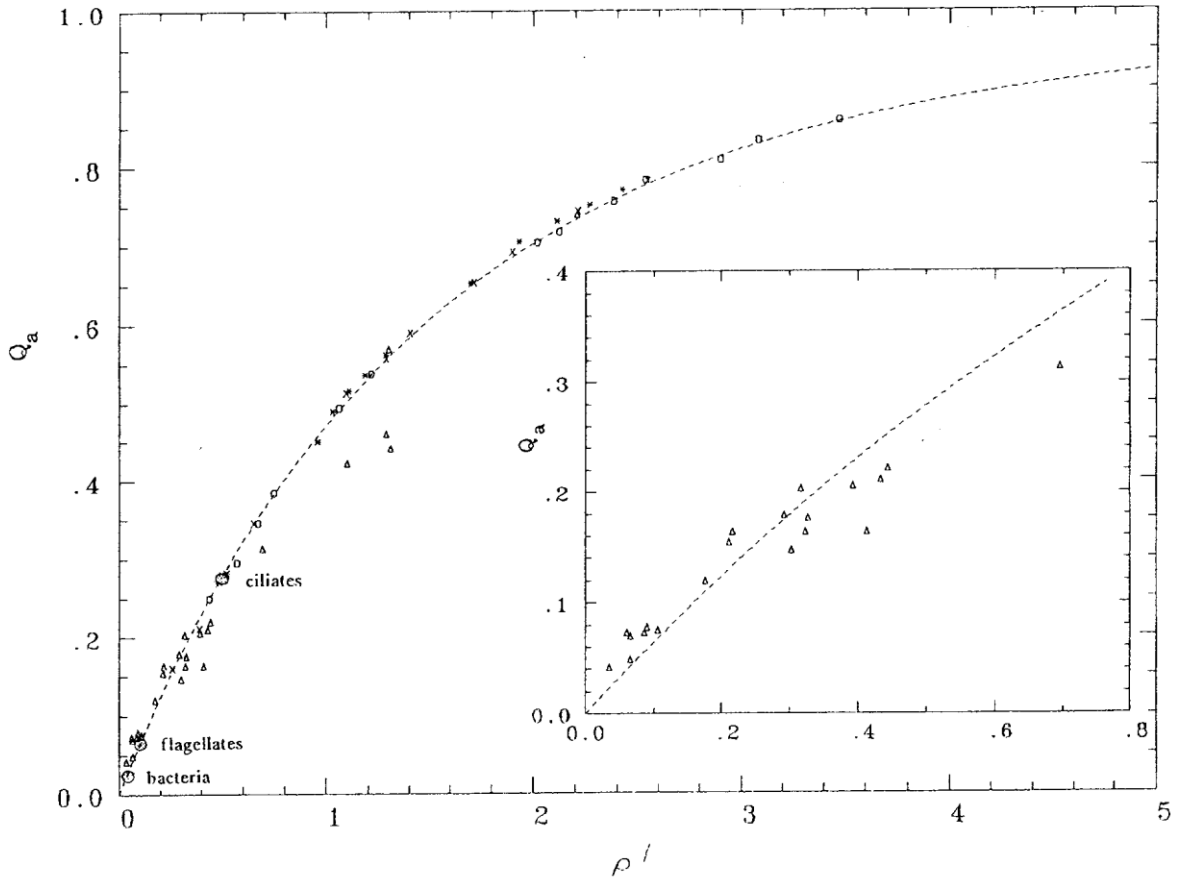

Figure 1. The theoretical variations of Q_a, the efficiency factor for absorption (dashed curves), as a function of the dimensionless parameter ρ',. The triangles are experimental determinations of Q_a (at 675 nm) for various algae (Morel and Bricaud, 1986; Ahn, 1990); other symbols are for determinations of 3 algal species studied by Sosik (1988). The values for heterotrophic organisms, as indicated, come from Morel and Ahn (1990, 1991). The inset is an enlargment of the initial part of the curve.

(Morel 1991)

Example spectra of absorption efficiency factor

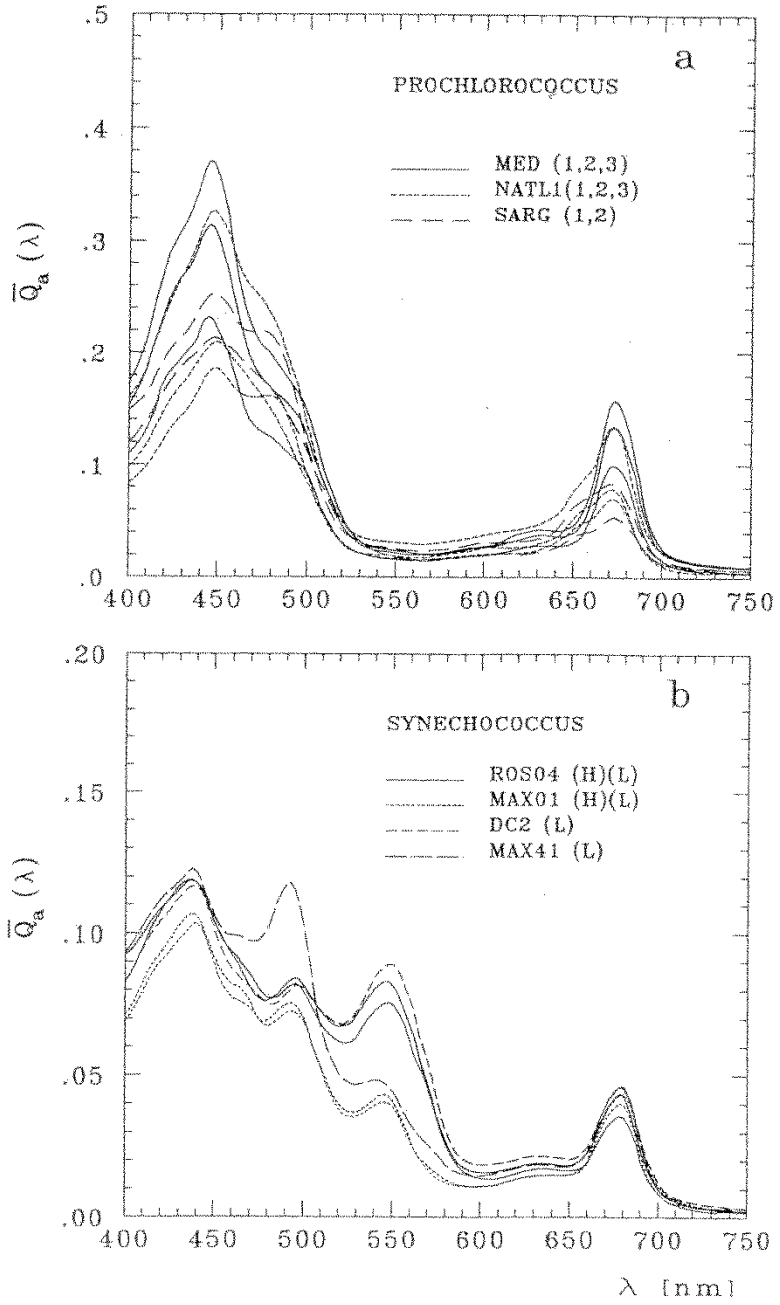

Figure 5. Spectral values of the efficiency factor for absorption for the various strains.

(Morel et al. 1993)

Particle size distributions of *Prochlorococcus* and *Synechococcus*

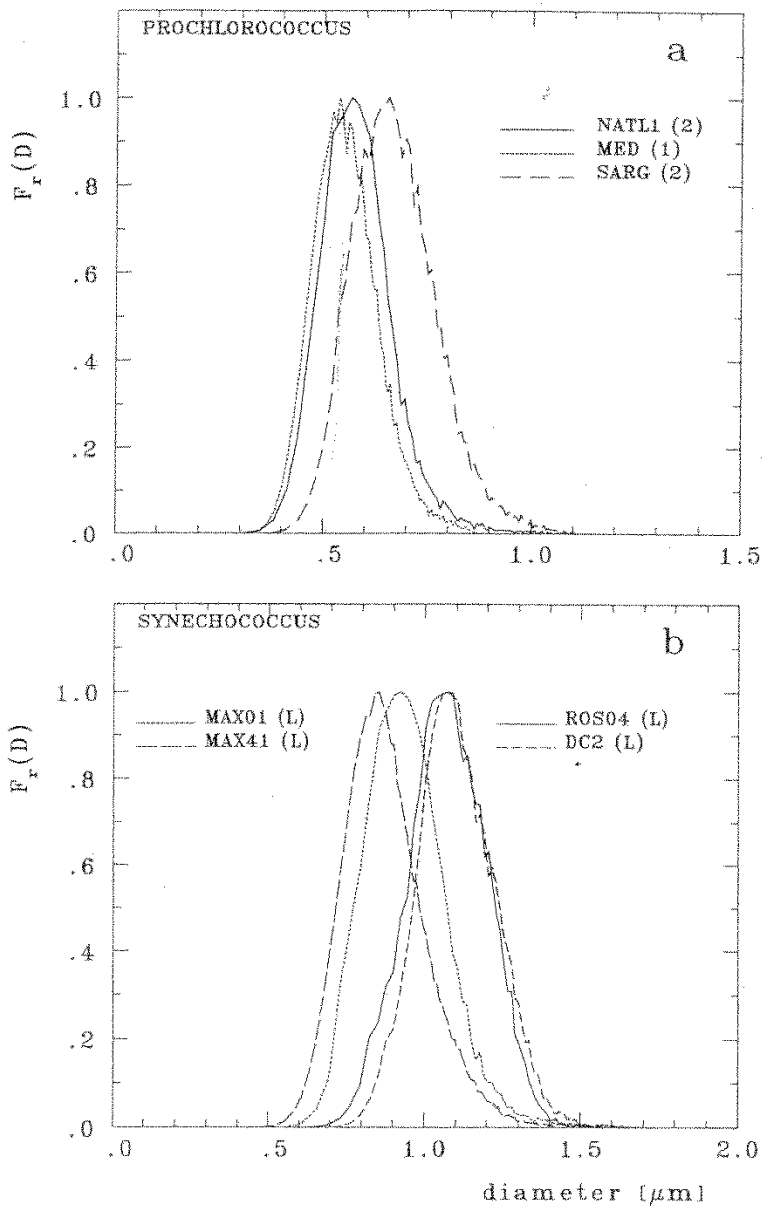

Figure 1. Relative size distribution functions (normalized to their maximum) for the various strains of *Prochlorococcus* (panel a) and *Synechococcus* (panel b), labelled as in Table 1. For clarity only one size distribution per strain is represented; the other curves, not shown, are almost identical apart from slight shifts of the maximum.

(Morel et al. 1993)

Scattering of light by inhomogeneity of the medium

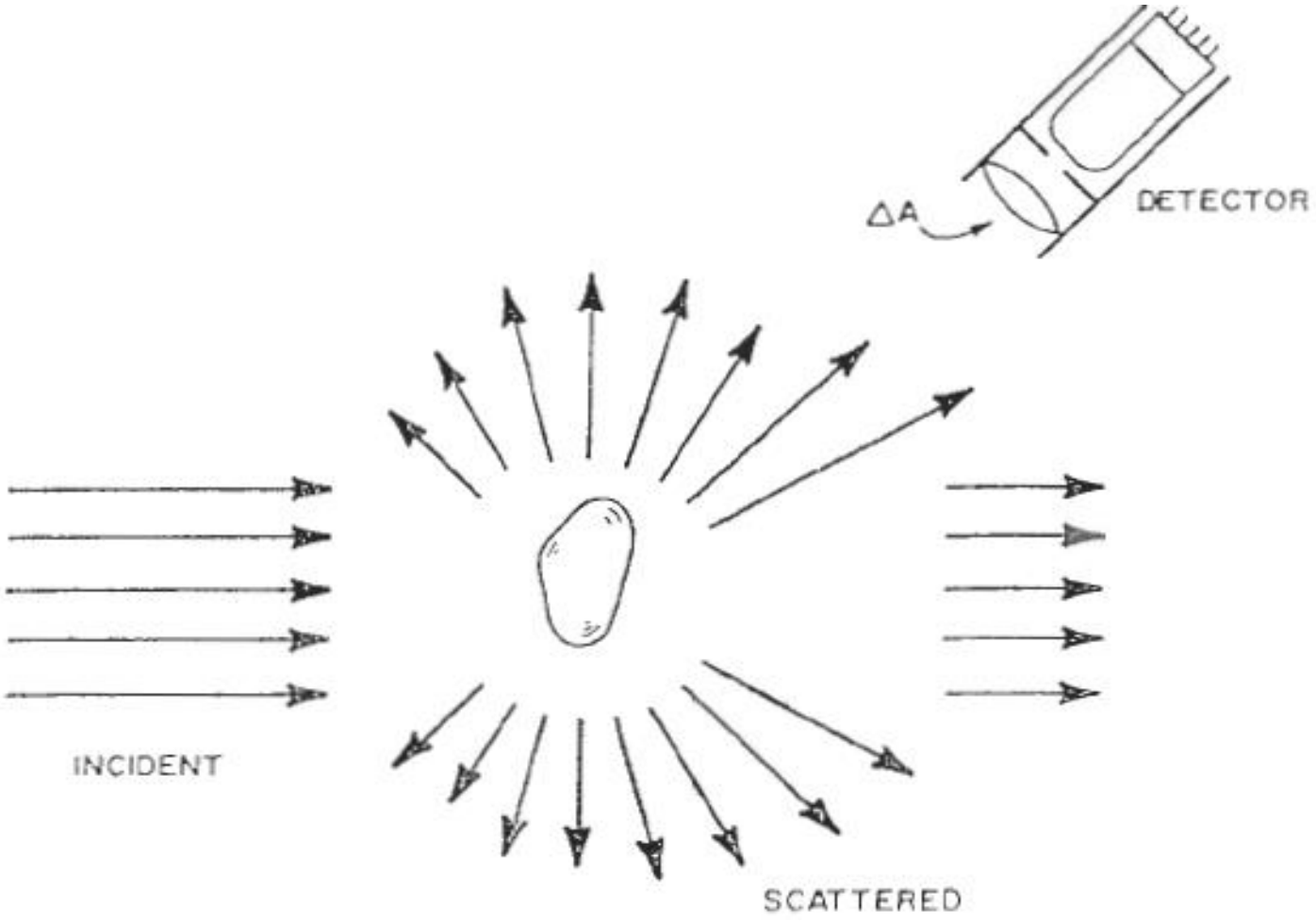

(Bohren and Huffman 1983)

Electromagnetic radiation of an oscillating dipole: Mechanism of light scattering

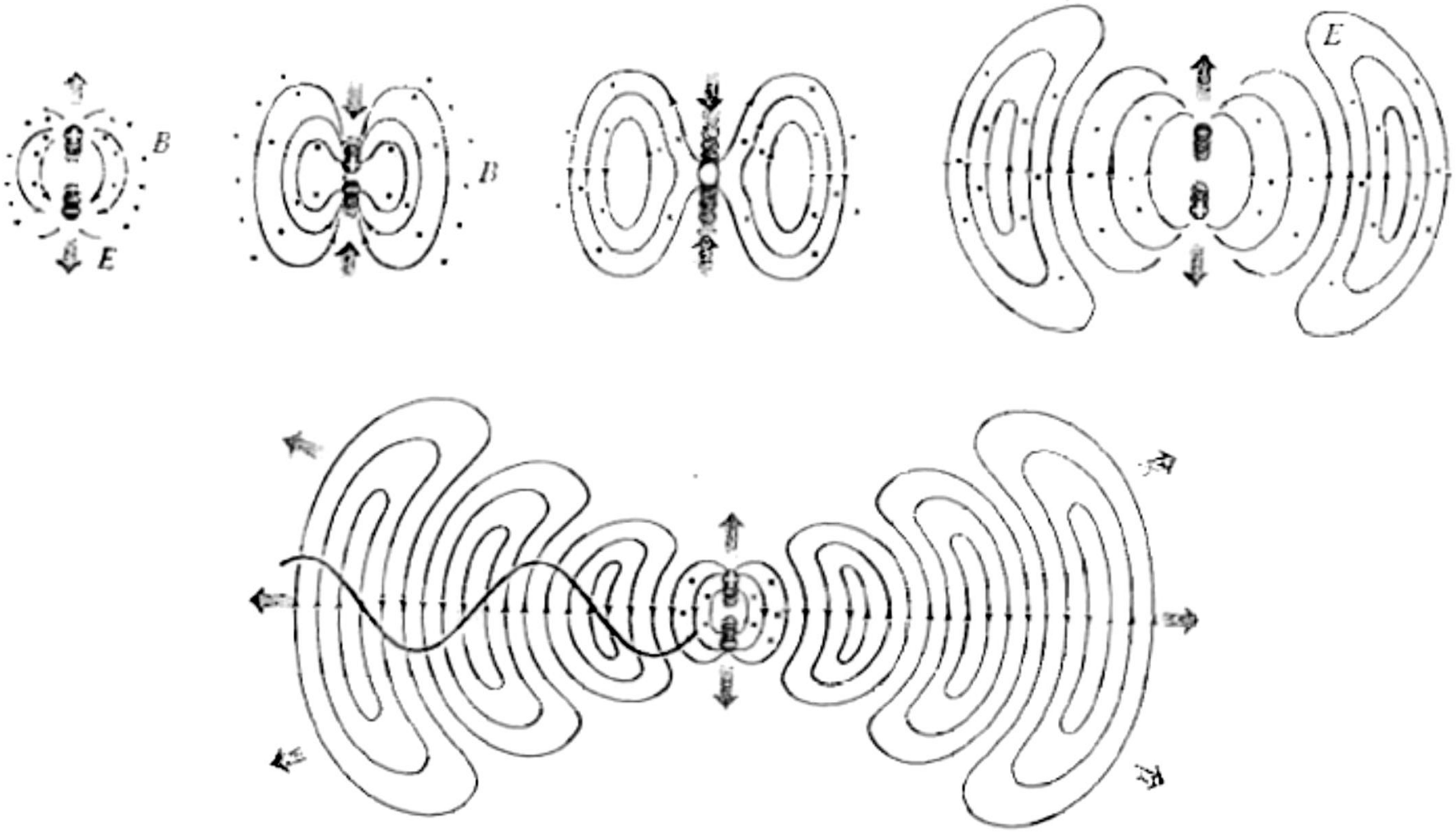

(Hecht 1994)

Inelastic scattering - Raman scattering

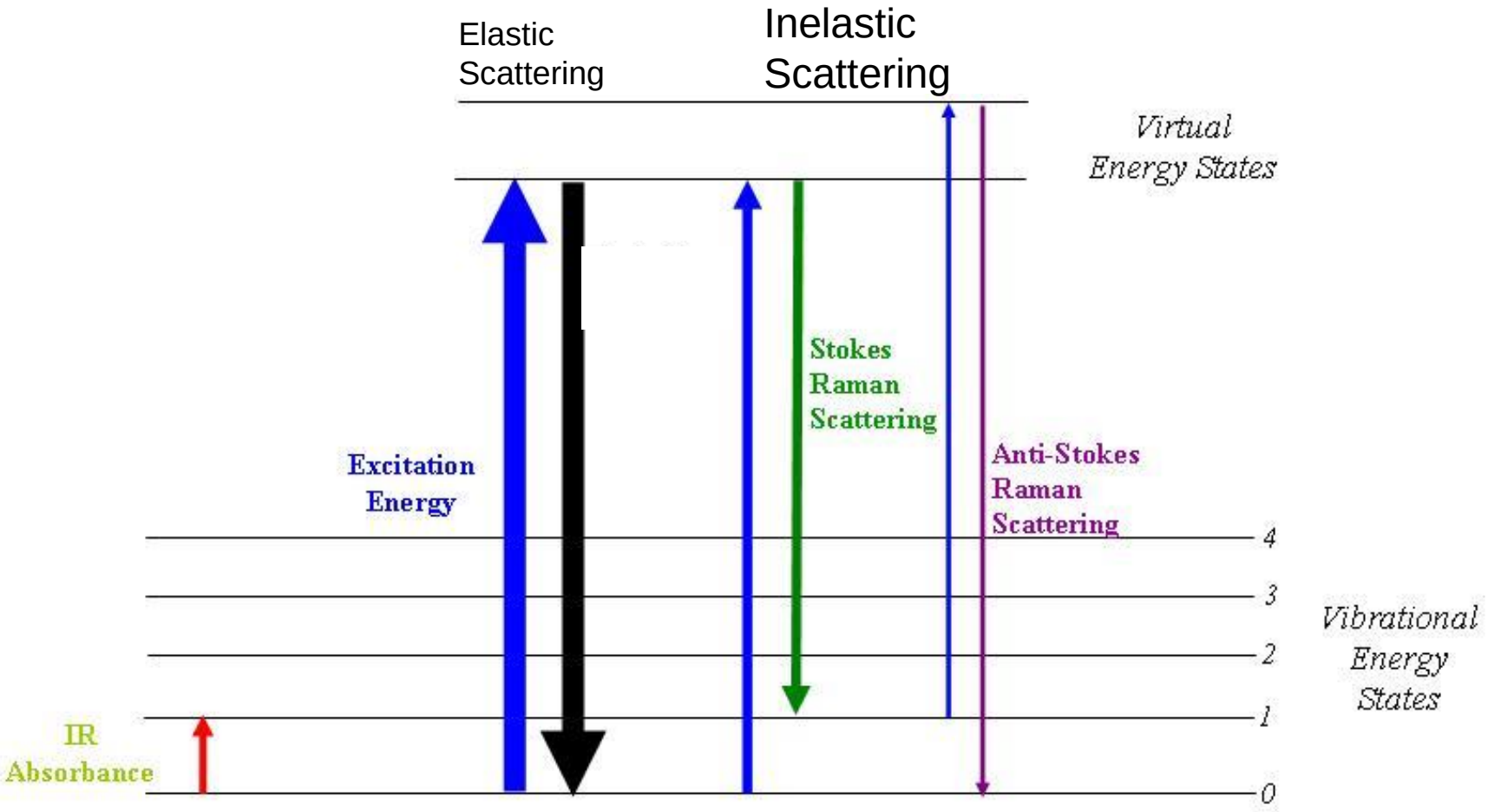

Dense homogeneous medium

Except for forward ($\psi = 0^o$) and backward ($\psi = 180^o$) directions the scattered radiation fields are 180^o out-of-phase and therefore interfere destructively

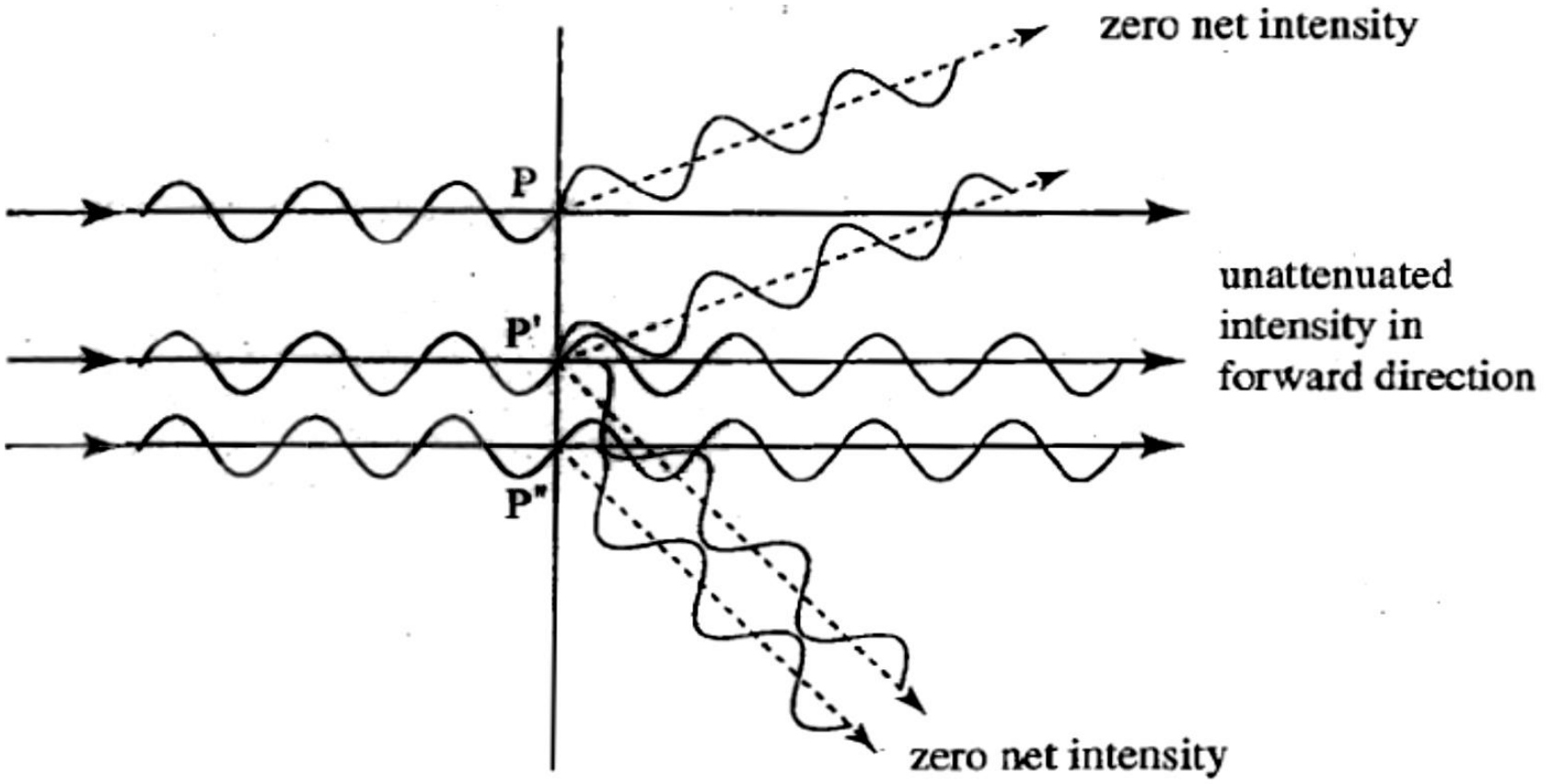

Small and large particle in the electric field of the electromagnetic wave

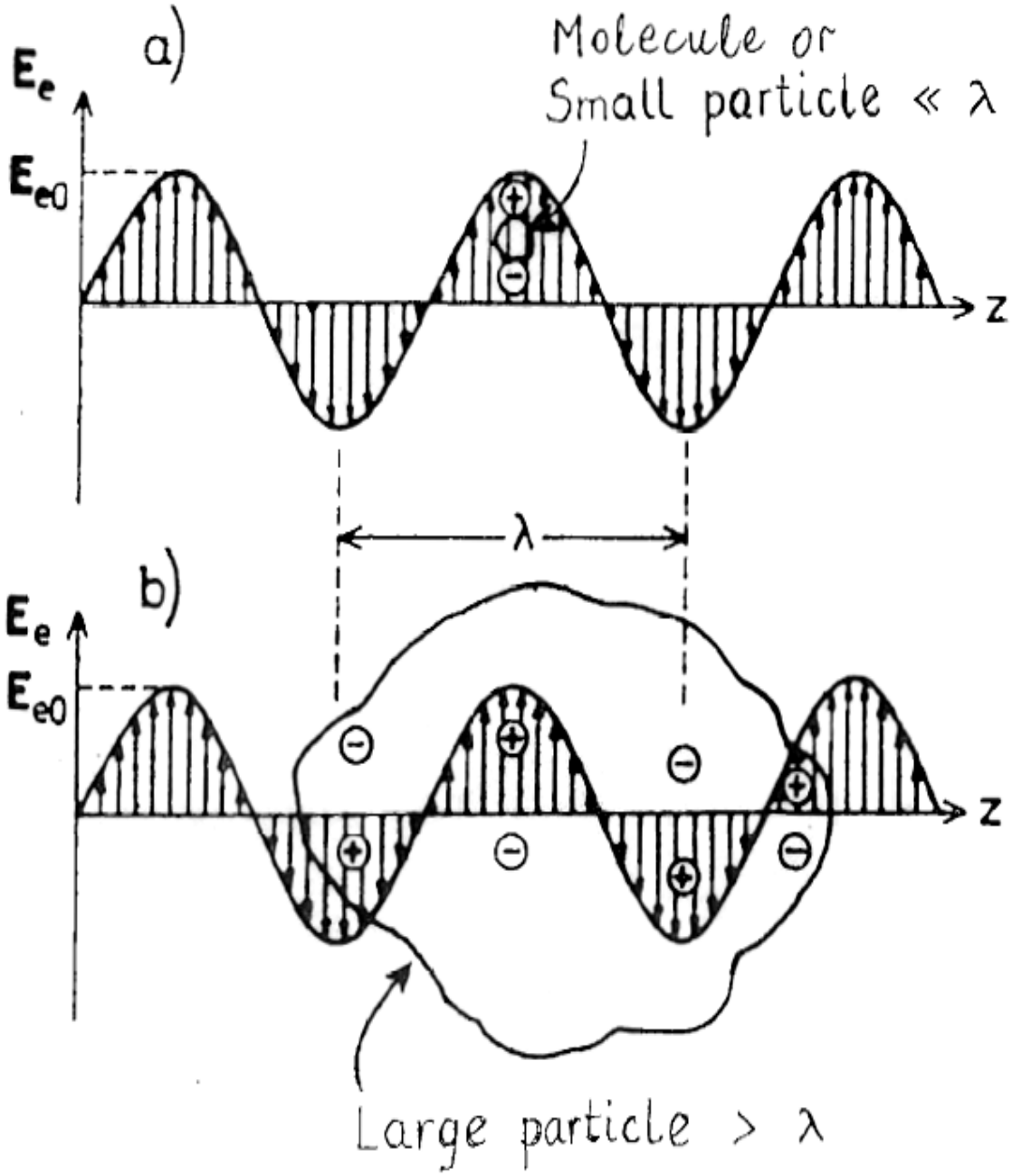

(Dera 1992)

A single particle subdivided into oscillating dipoles

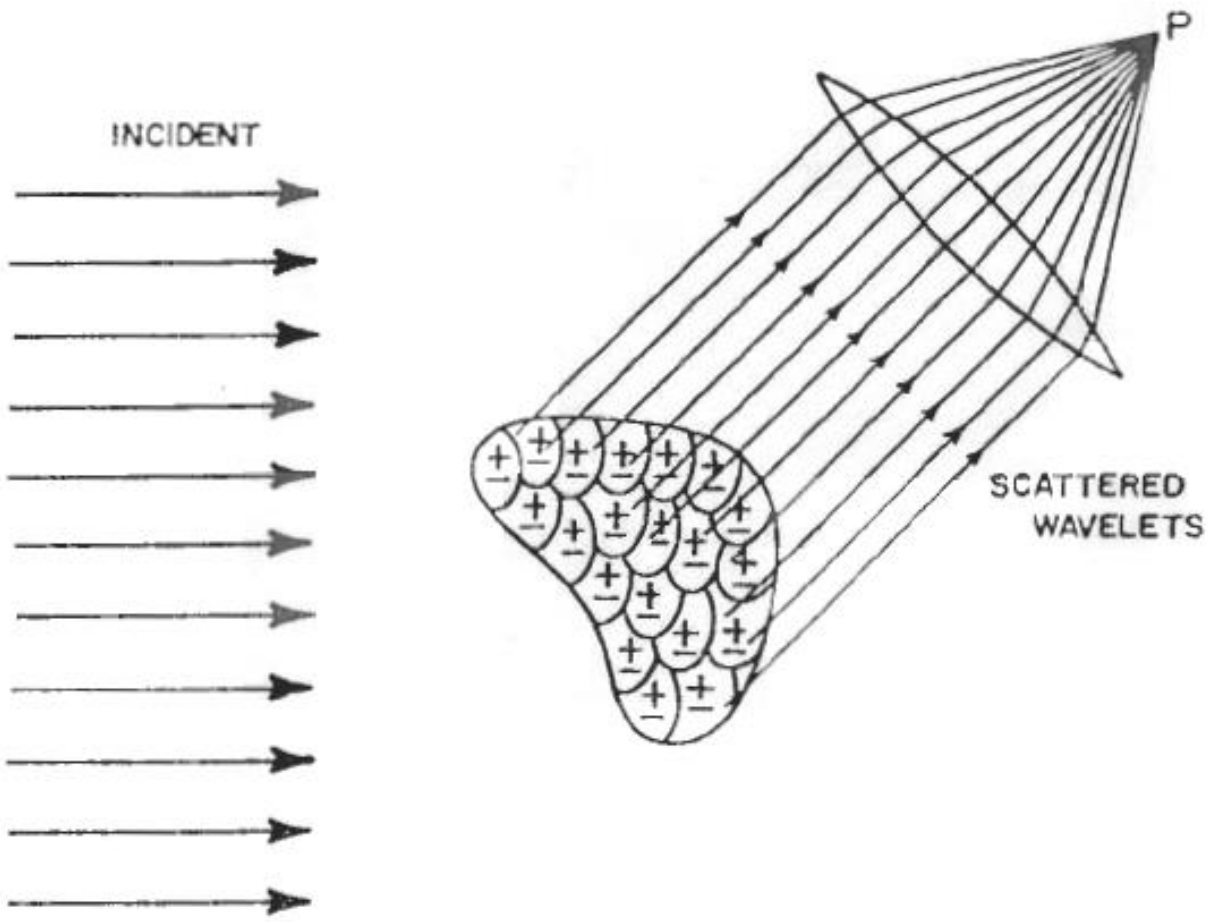

(Bohren and Huffman 1983)

The interference pattern produced by two slits

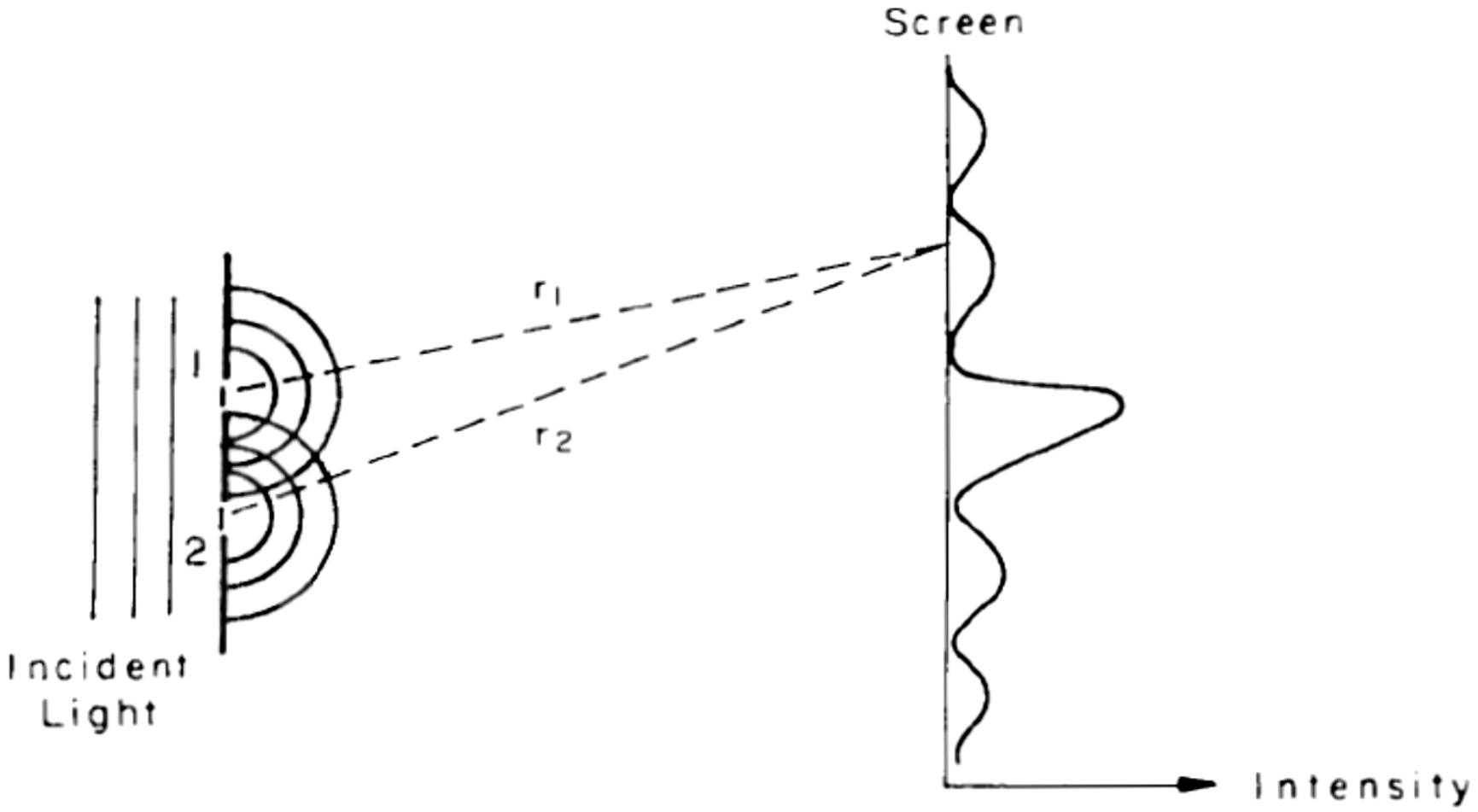

Angular patterns of scattered intensity from particles of different sizes

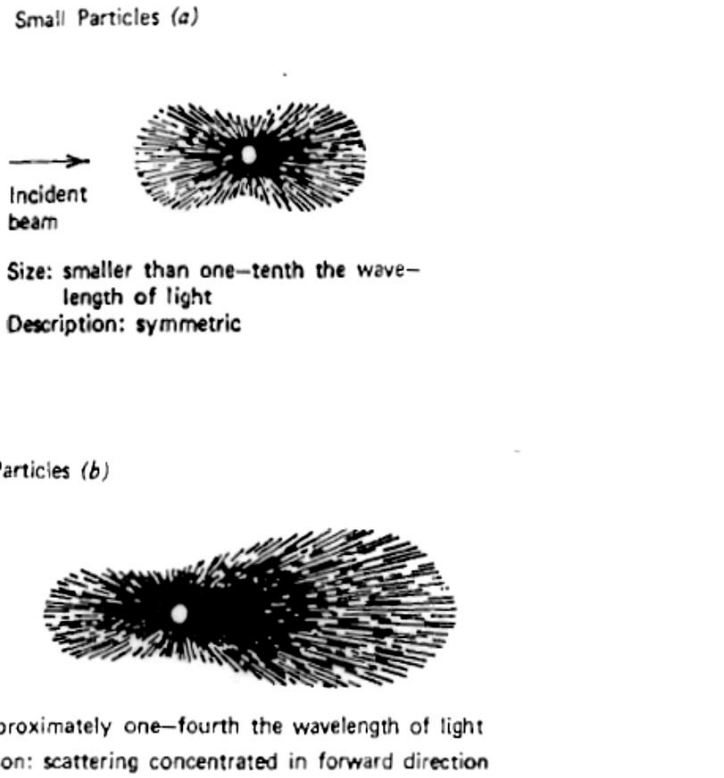

(McCartney 1976)

Molecular scattering as a function of light wavelength

Scattered Intensity ~ λ^{-4}

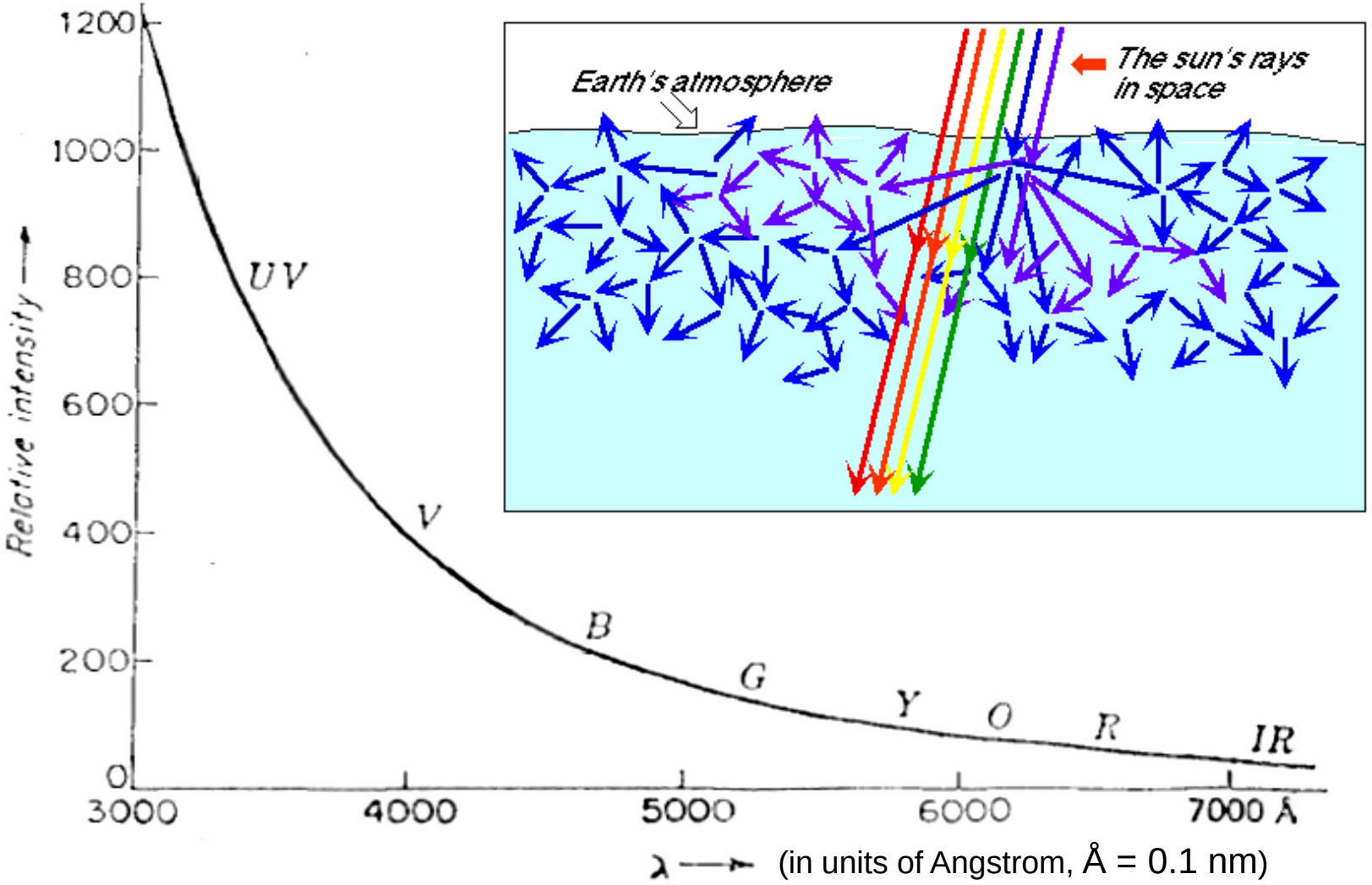

Geometric ray tracing approach

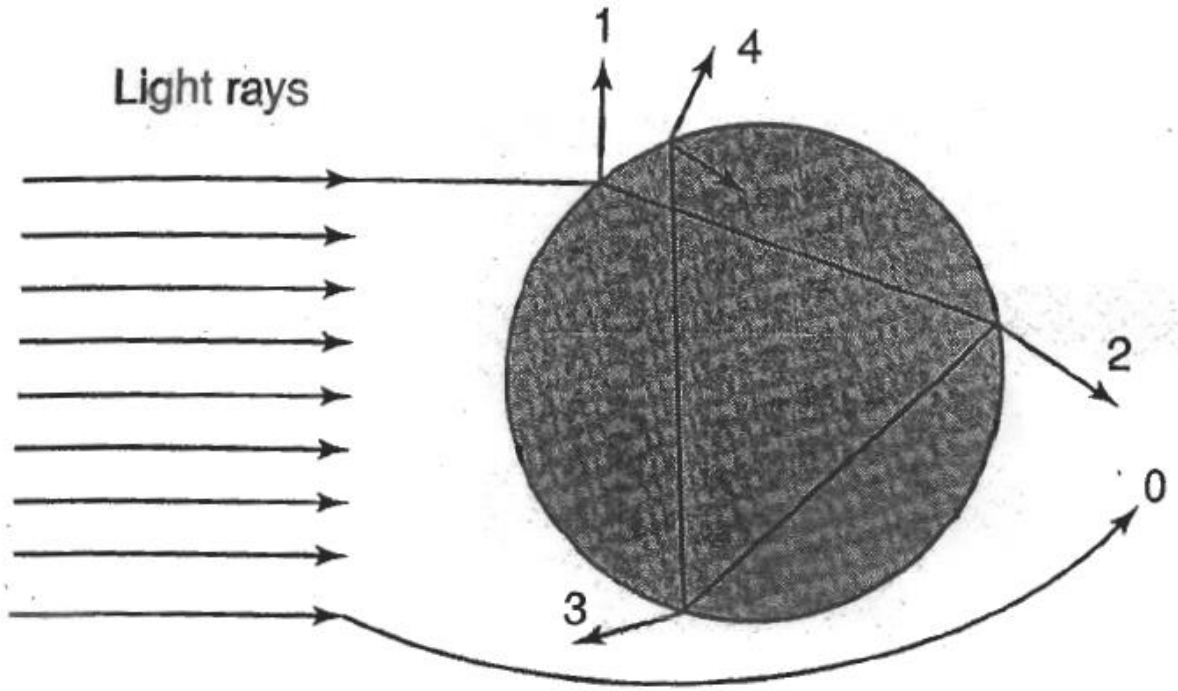

0 Exterior Diffraction

1 External Reflection

2 Two Refractions

3 One Internal Reflection

4 Two Internal Reflections

Diffraction

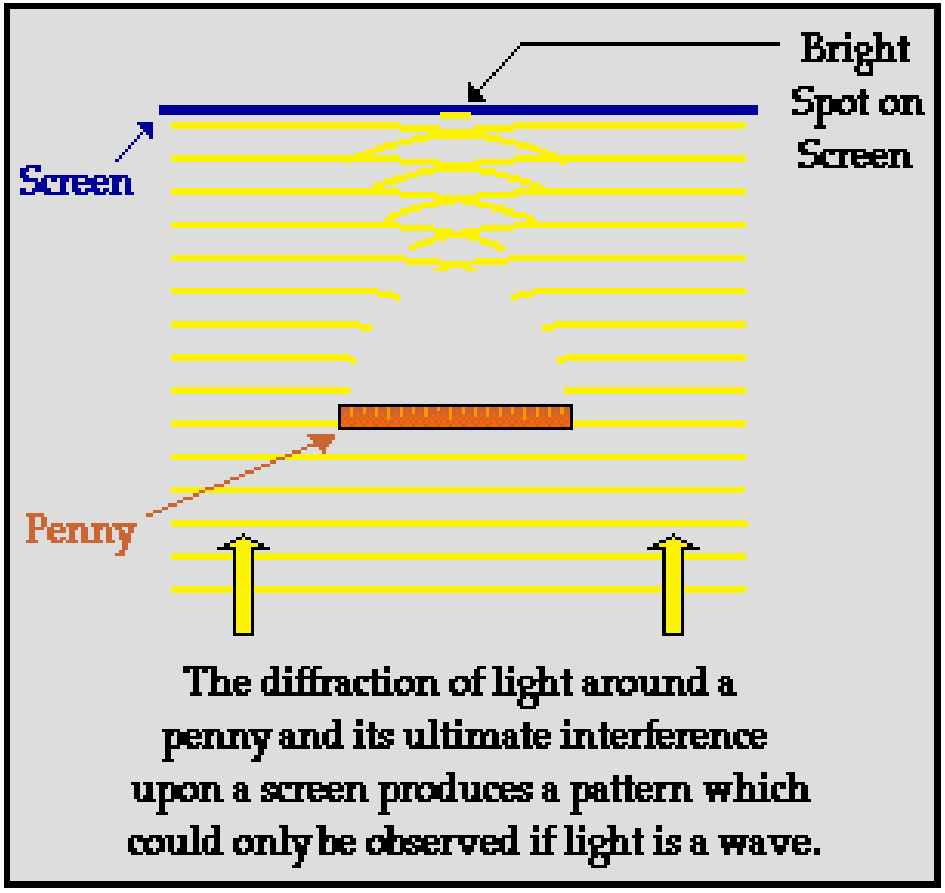

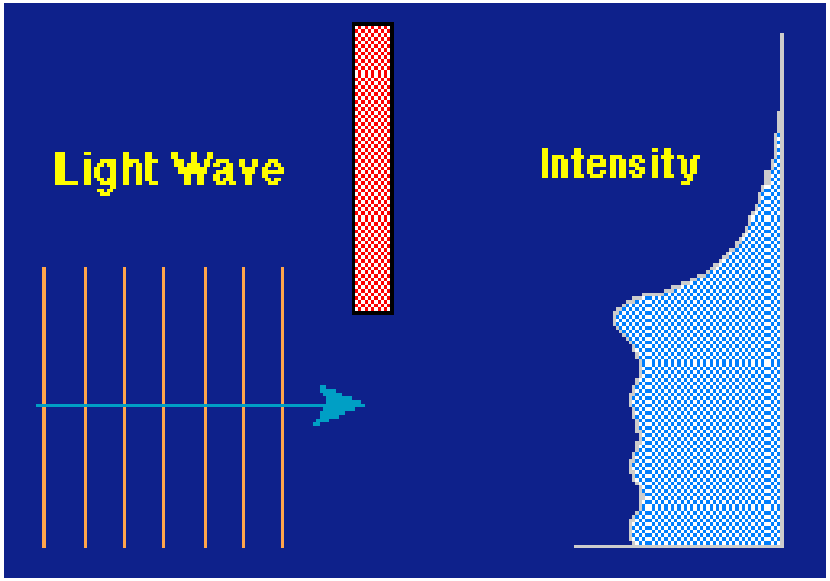

The intensity of light behind the barrier is not zero in the shadow region due to diffraction (light wave has a capability to “bend around corners”)

Scattering by a collection of particles

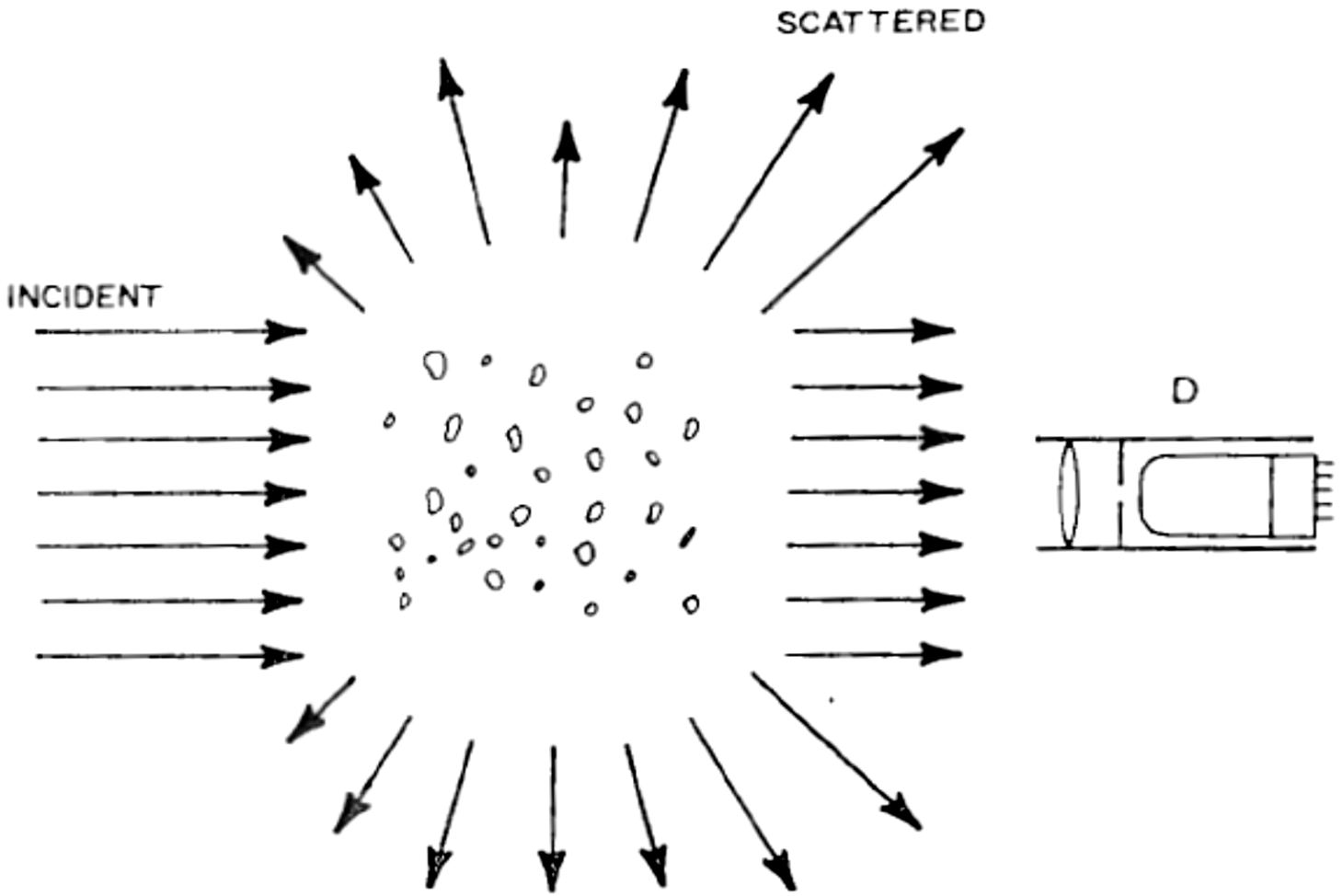

(Bohren and Huffman 1983)

Multiple light scattering by a collection of particles

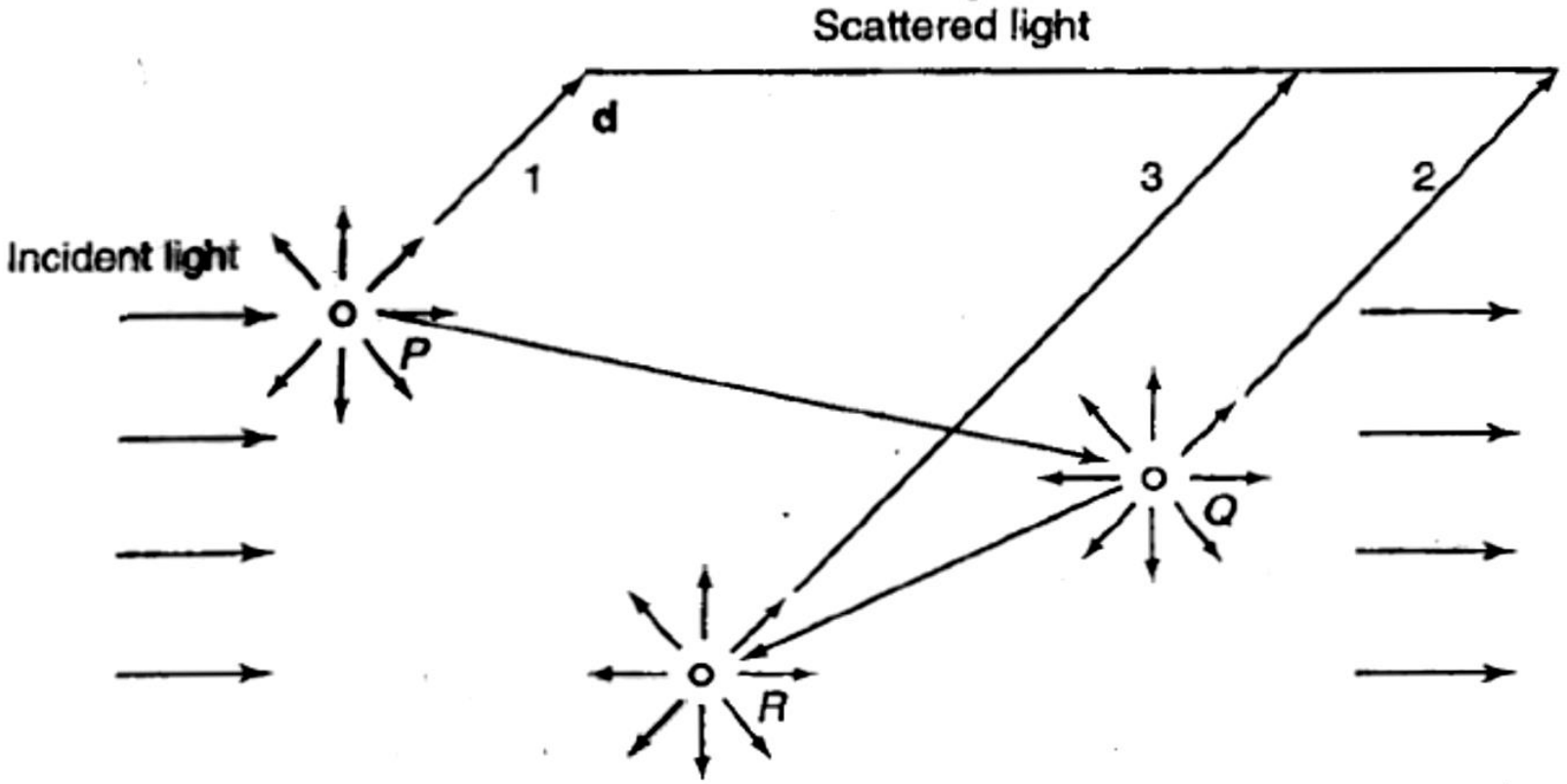

Figure 1.5 Multiple scattering process involving first (P), second (Q), and third (R) order scattering in the direction denoted by **d**.

(Liou 2002)

Scattering by a single particle: Phase shift parameter

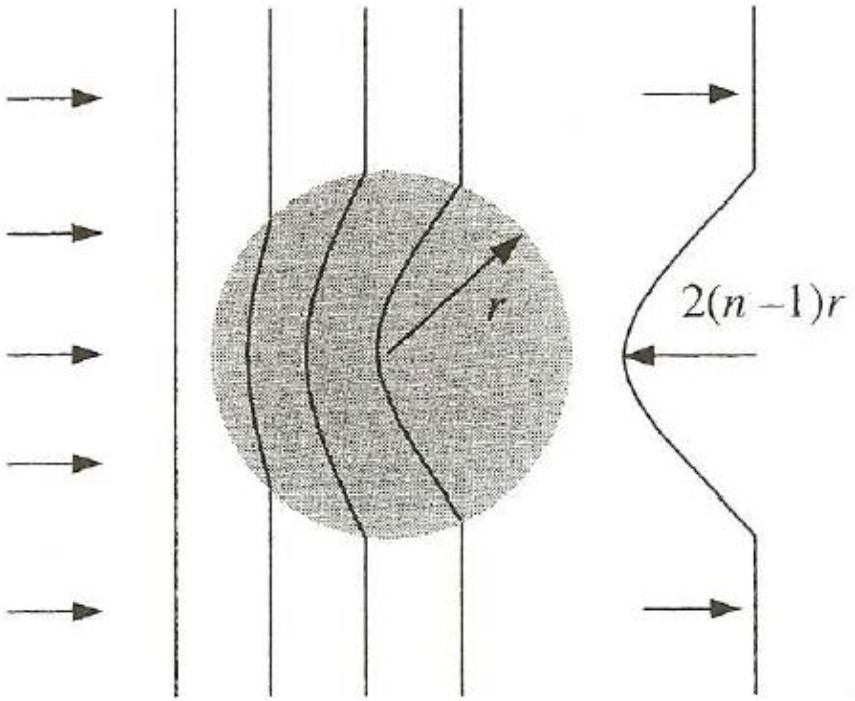

Figure 3.5. Phase fronts of a light wave traveling through a sphere of radius r. The wave slows down while traveling through the particle. The accumulated phase difference is proportional to the total distance traveled through the particle and is a function of the point of entry. The phase difference between the light passing through the center of the sphere and the light passing outside the sphere is $2(n-1)r$.

(Jonasz and Fournier 2007)

Optical efficiency factors versus phase shift parameter

phase shift parameter $\rho = 2\,\alpha\,(n-1)$

$Q_a = F_a/F_o$ $Q_b = F_b/F_o$ $Q_c = F_c/F_o$

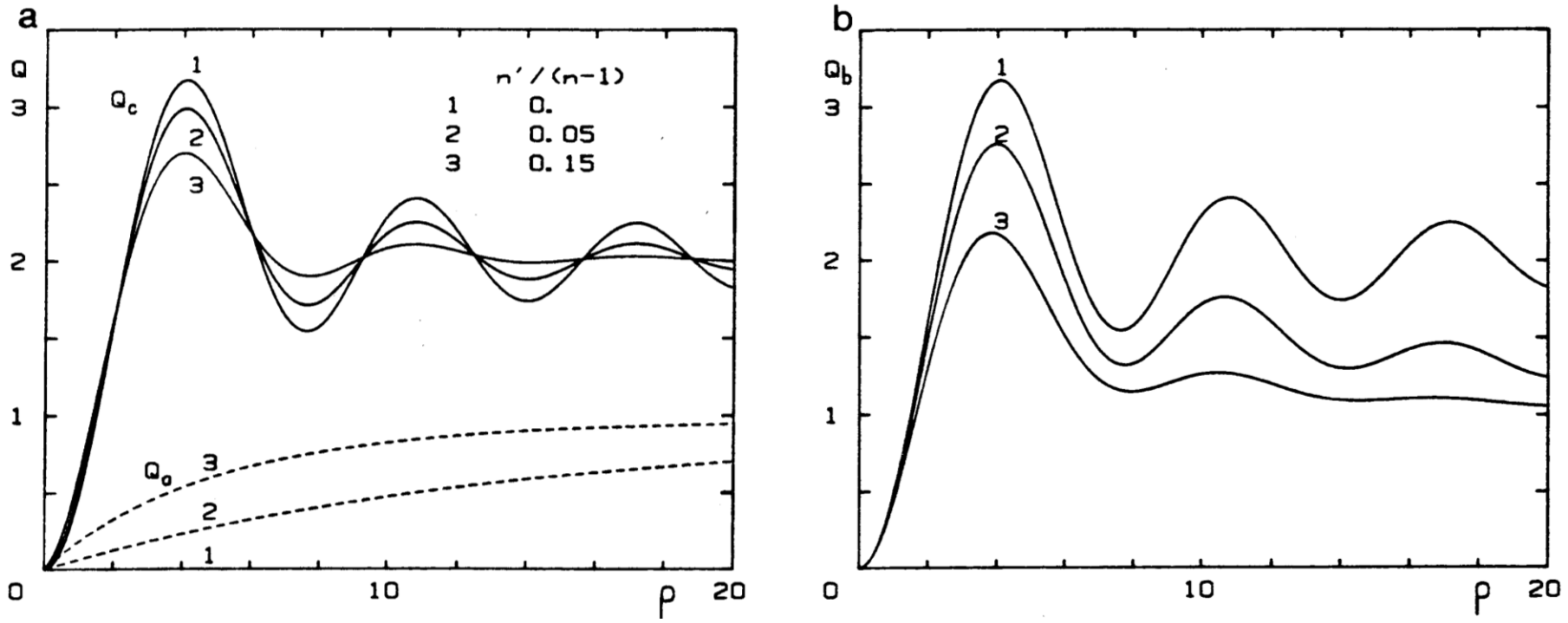

FIG. 3. Variations of the efficiency factors for attenuation, Q_c, *for absorption,* Q_a (a), and for scattering, Q_b (b) vs. the parameter $\varrho = 2\,\alpha(n-1)$, for increasing values of the ratio $n'/(n-1)$ where n and n' are the real and imaginary parts of the relative refractive index of the particles.

(Morel and Bricaud 1986)

The effect of polydispersion on attenuation efficiency

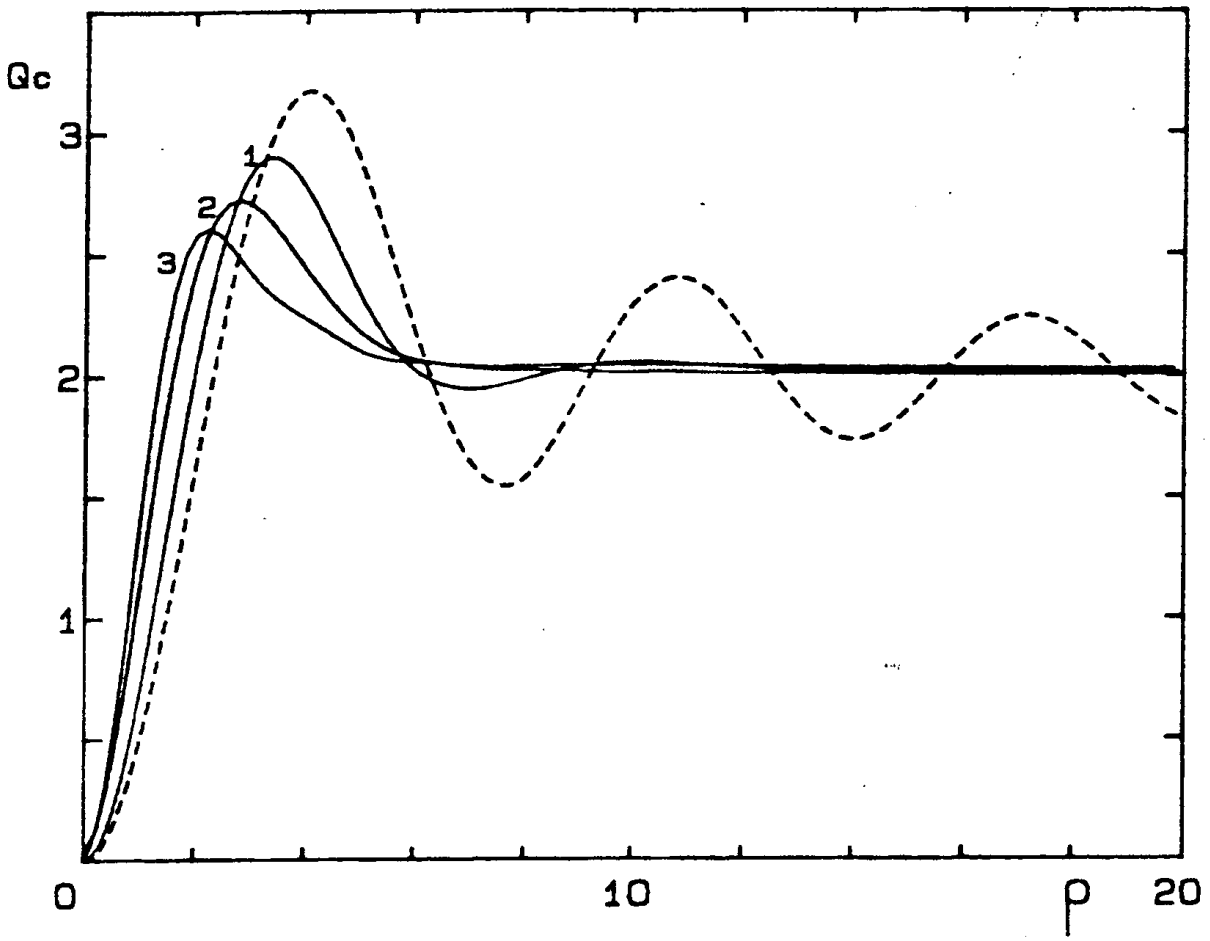

FIG. 4. Mean efficiency factor for attenuation Q_c of a "mean" particle representative of a polydispersed population, plotted as a function of ϱ_m, *the* ϱ value which corresponds to the maximum of the size distribution function $F(\varrho)$ (see Equation 17). The index of refraction is real (no absorption) and the curves 1 and 3 correspond to log-normal distributions such as $F(\varrho_M/2) = F(2\varrho_M) =$ respectively 0.01, 0.1, 0.3 $F(\varrho_M)$. The dashed curve, redrawn from Fig. 3 for $n' = 0$, represents the limiting case of a population of monosized particles.

(Morel and Bricaud 1986)

Scattering and backscattering efficiencies versus particle size

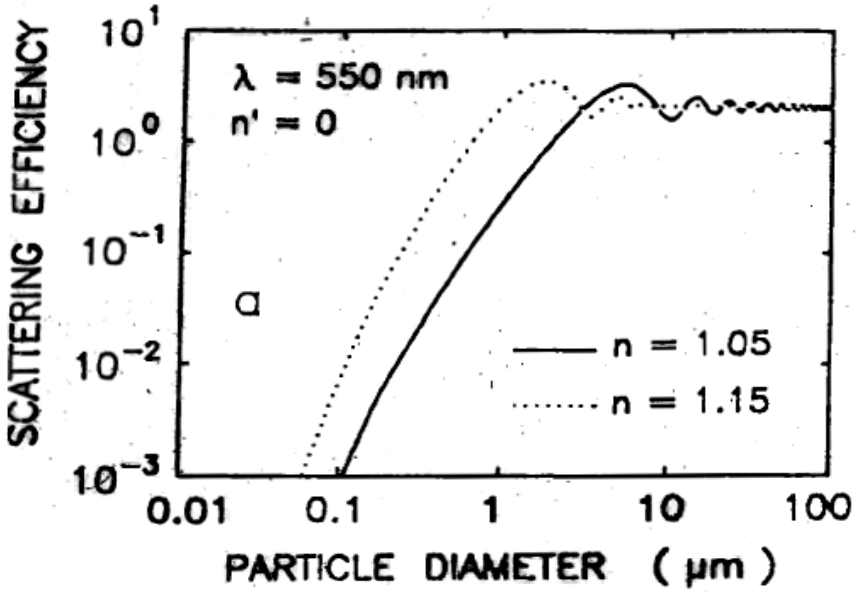

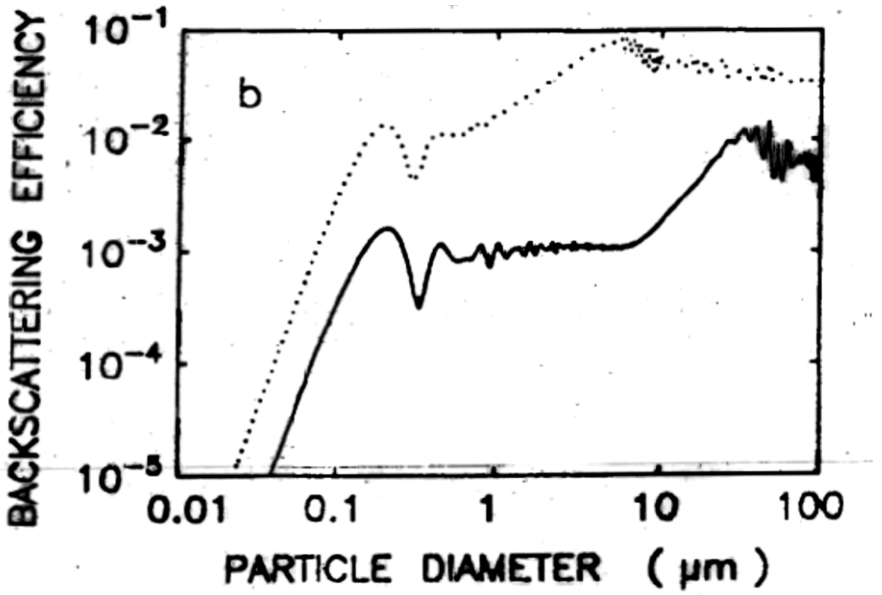

(Stramski and Kiefer 1991)

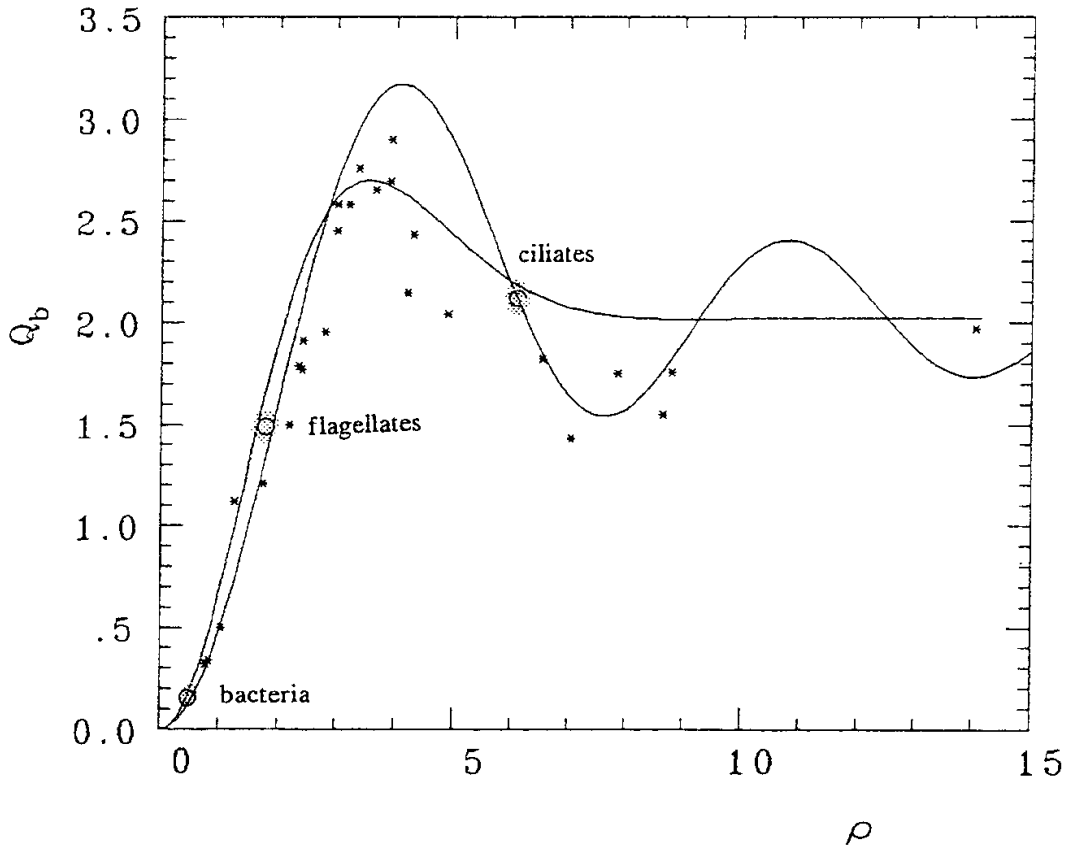

Figure 2. The theoretical variations of Q_b , the efficiency factor for scattering by non absorbing spheres (solid curve with marked oscillations) as a function of the dimensionless parameter ρ. The smoothed curve is for an averaged $\bar{Q}_b$ to be applied for population with a log - normal size distribution. The crosses are the $\bar{Q}_b$ values (at $\lambda \sim 580$ nm) determined for various phytoplankters grown in culture (see Table 1 in Morel and Bricaud, 1986); additional data for algal cells come from Ahn (1990). The circles indicate the $\bar{Q}_b$ values (at $\lambda \sim 550$ nm) determined for free living marine bacteria, heterotrophic flagellates, and naked ciliates, (Morel and Ahn, 1990; 1991).

(Morel 1991)

Spectra of scattering efficiency for various phototrophic and heterotrophic microorganisms

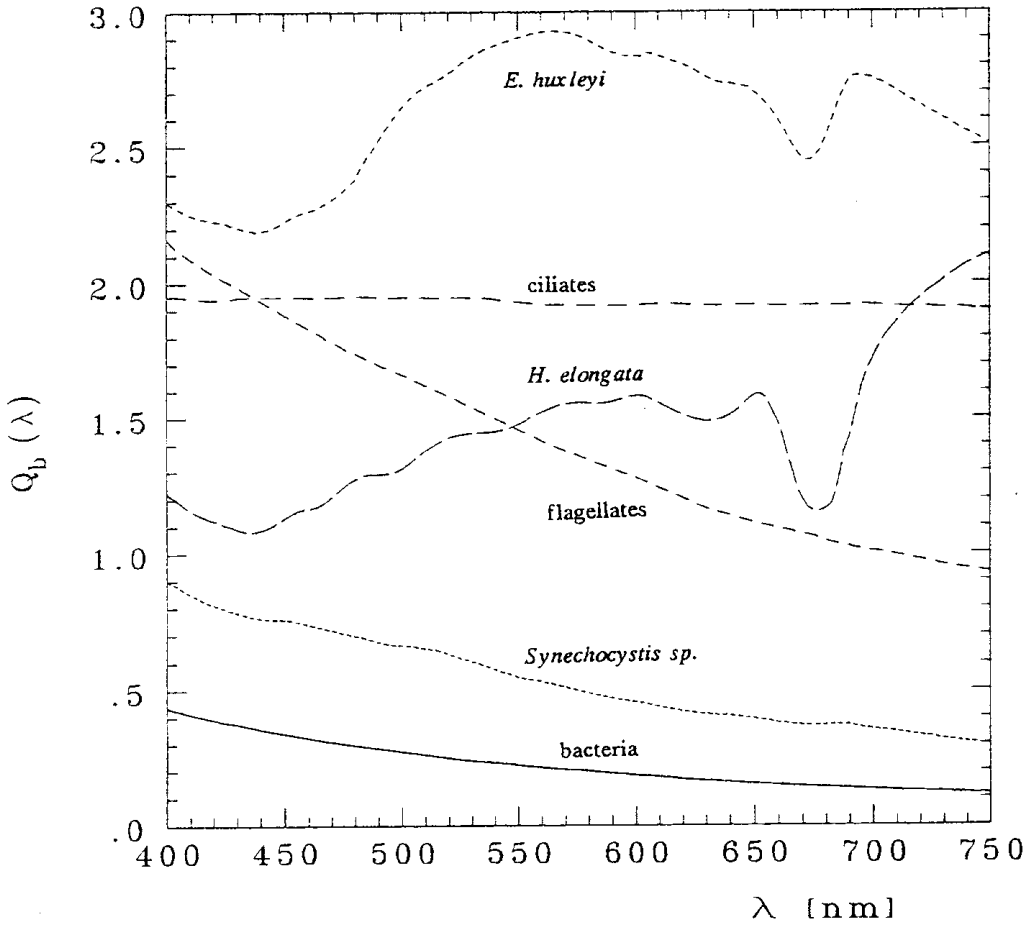

Figure 3. Spectral variations of Q_b within the 400-750 nm range of various phototrophic and heterotrophic organisms as experimentally determined (Morel and Ahn, 1990, 1991).

(Morel 1991)

Anomalous dispersion of the refractive index within the absorption band

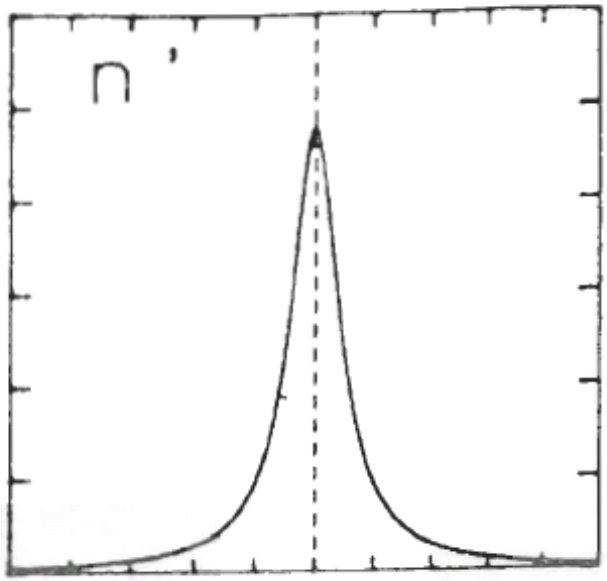

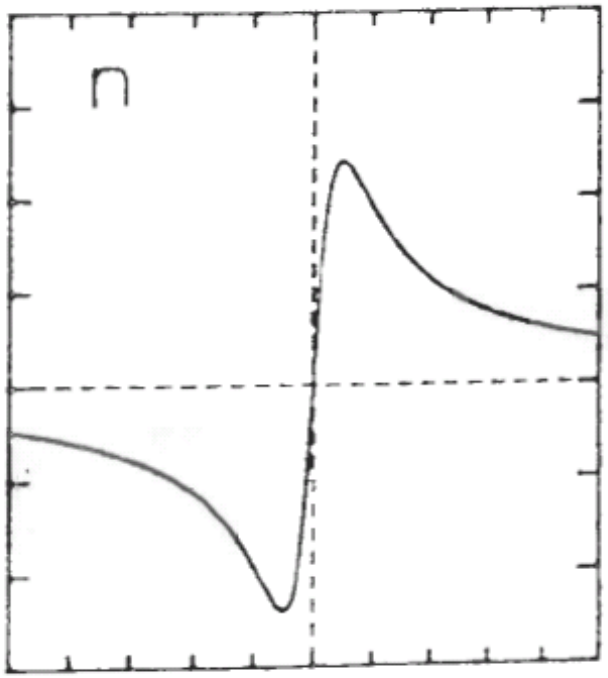

(Morel and Bricaud 1986)

Optical efficiency factors:

Examples for monospecific cultures of algal cells

(deduced from the absorption and attenuation coefficients, and size distribution measurements)

$\bar{d} \simeq 3.4\ \mu m$
$n \simeq 1.07$
$\alpha \simeq 20 \ldots 35$
$\rho \simeq 3 \ldots 5$
for the visible light

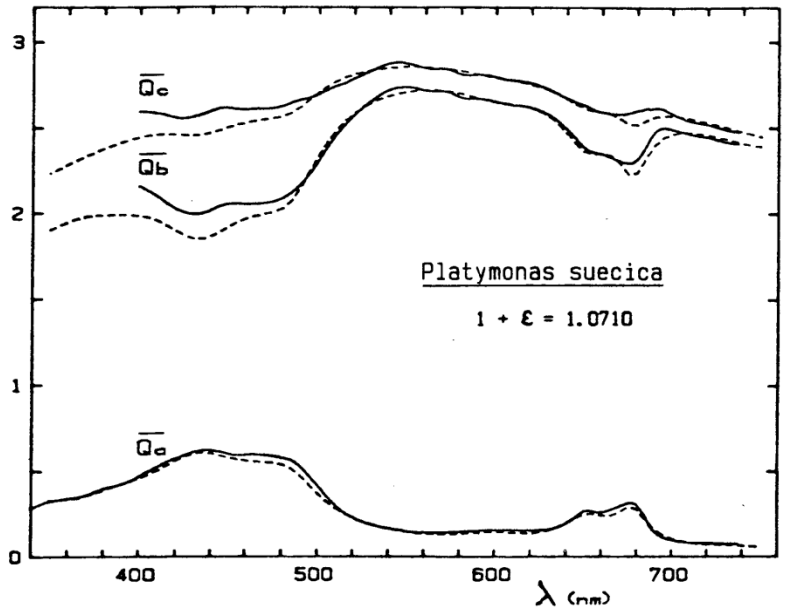

$\bar{d} \simeq 1.2\ \mu m$
$n \simeq 1.05\ \mu m$
$\alpha \simeq 7 \ldots 13$
$\rho \simeq 0.5 \ldots 1.5$
for the visible light

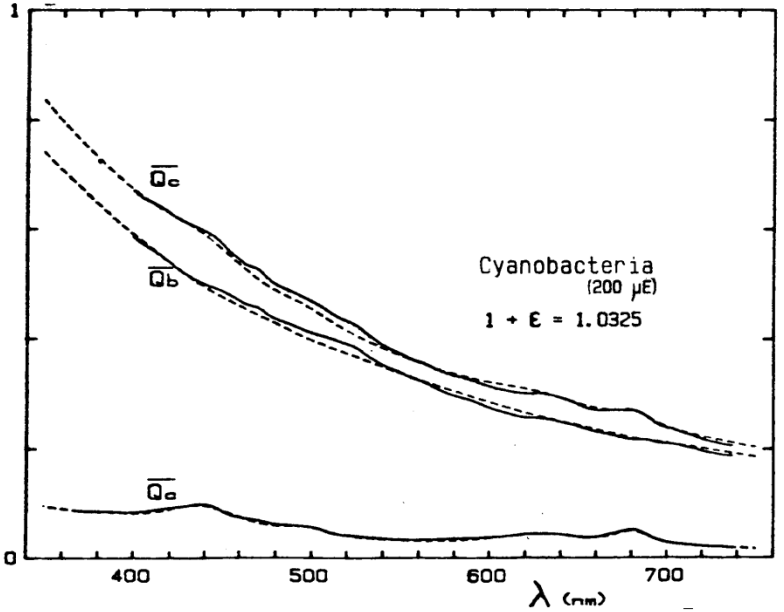

FIG. 14. Spectral variations of the mean efficiency factors for attenuation ($\bar{Q}_c$), scattering ($\bar{Q}_b$) and absorption ($\bar{Q}_a$), deduced from the attenuation and absorption coefficients experimentally determined (continuous lines), for two phytoplanktonic species. The variations of $\bar{Q}_c$, $\bar{Q}_b$ and $\bar{Q}_a$ obtained from a theoretical model (see text) are shown as dashed lines. The central value of the real part of the refractive index, $1 + \epsilon$, leading to the best theory/experiment agreement is indicated on the Figures.

(Morel and Bricaud 1986)

Scattering phase function: Effect of polydispersion

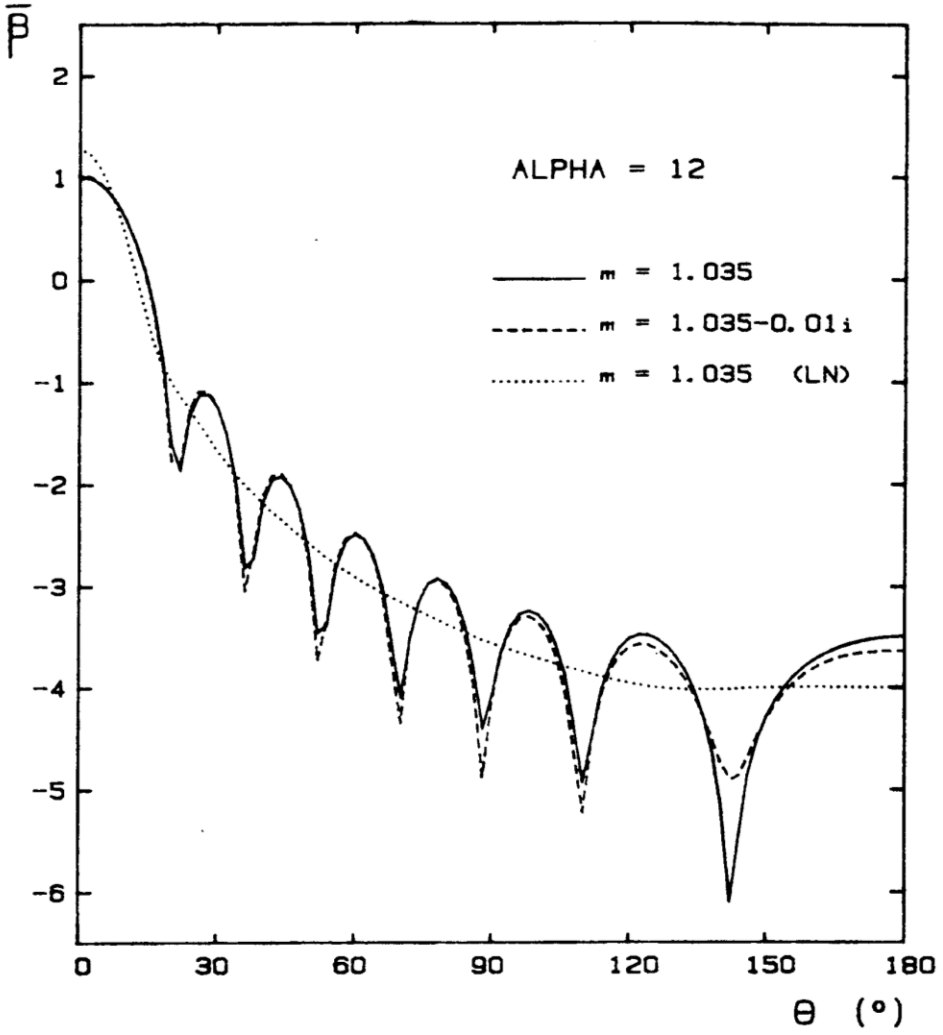

FIG. 5. Normalized volume scattering functions, $\beta(\theta)$ (Equations 5′ and 18), for a particle of relative size $\alpha = 12$, when the refractive index is 1.035 and 1.035–0.01 i. The dotted curve represents the same $\bar{\beta}(\theta)$ function for a polydispersed population of particles with $n = 1.035$, computed according to Equation 20. The size distribution function $F(\alpha)$ is a log-normal law such that the modal relative size $\bar{\alpha}_M$ is also 12, and $F(\alpha_M/2) = F(2\alpha_M) = 0.01\ F(\alpha_M)$.

(Morel and Bricaud 1986)

Scattering phase function: Effects of particle size and refractive index

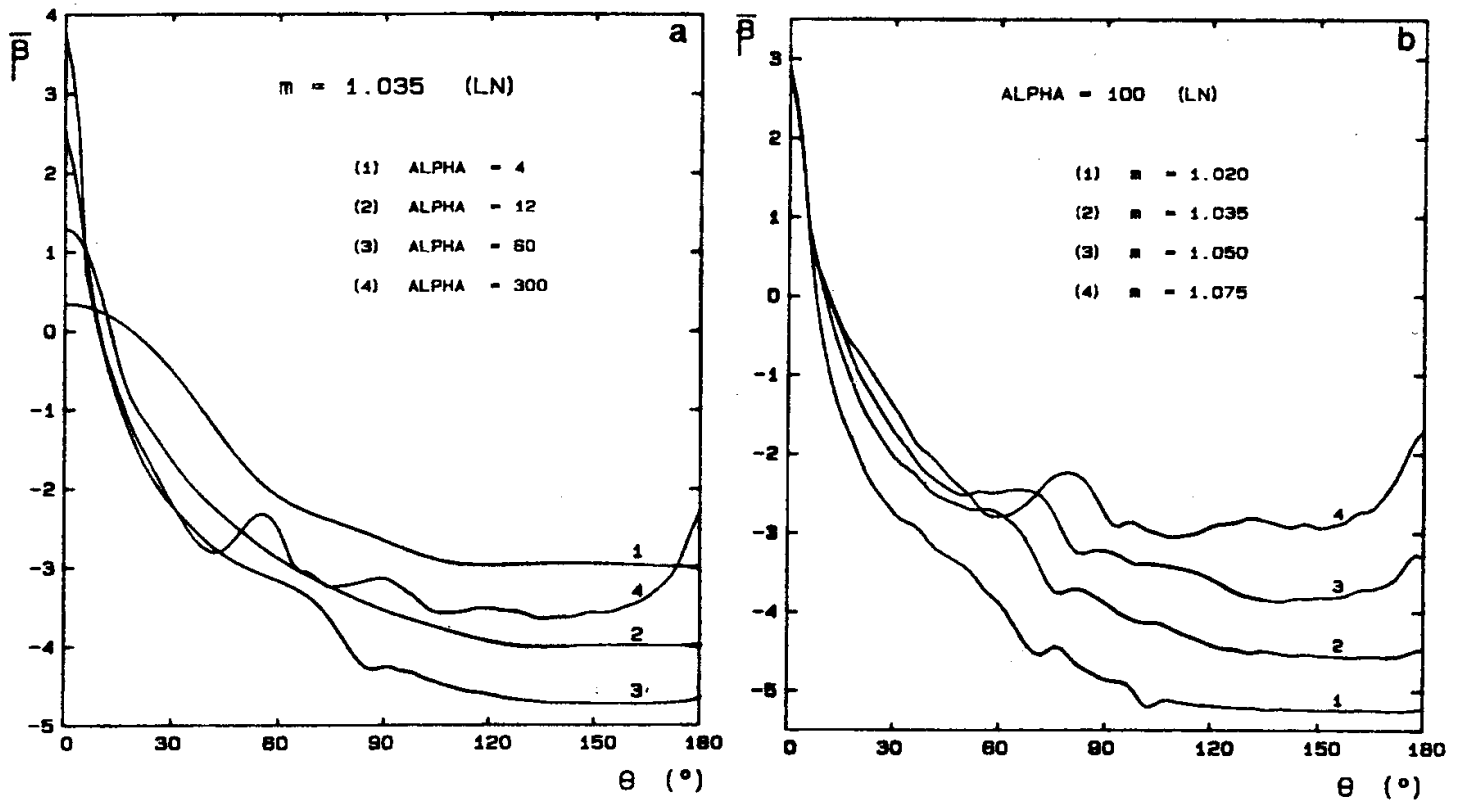

FIG. 6. (a) Normalized volume scattering function $\bar{\beta}(\theta)$ for increasing α_M values (increasing size) and for $m = 1.035$. (b) Normalized volume scattering function $\bar{\beta}(\theta)$ for increasing (real) index of refraction and for $\alpha_M = 100$. For Fig. 6a and b the log normal size distribution used is as in Fig. 5. The "bump" which occurs at about 75° for $m = 1.075$ and at smaller angles when the refractive index decreases (see also Fig. 6a) is the first "rainbow", at 138° for water droplets ($n = 1.33$). It appears for sufficiently large and perfect spheres. Thus it is unlikely that it can be observed for algal cells.

(Morel and Bricaud 1986)

Normalized scattering function for various microorganisms (from Mie calculations)

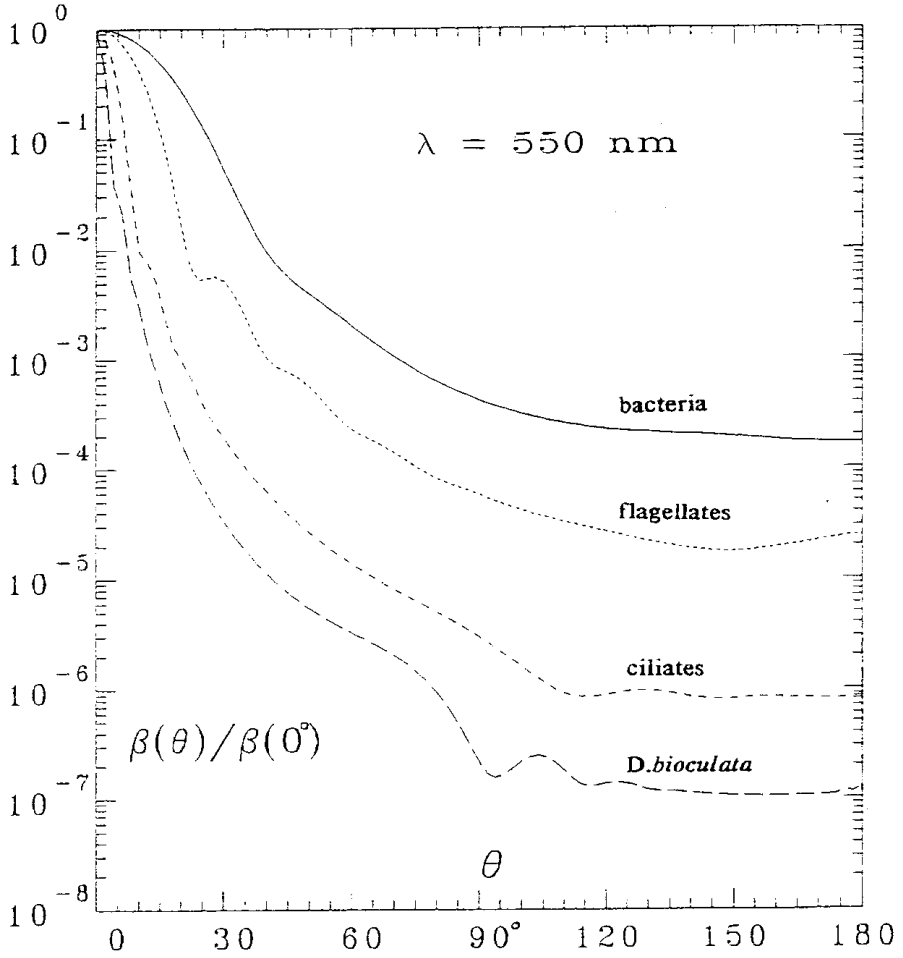

Figure 6. Volume scattering function (normalized at $\theta = 0°$ and for $\lambda = 550$ nm) computed for various organisms by using their refractive index and size distribution as experimentally determined (see text).

(Morel 1991)

Backscattering ratio versus relative size parameter

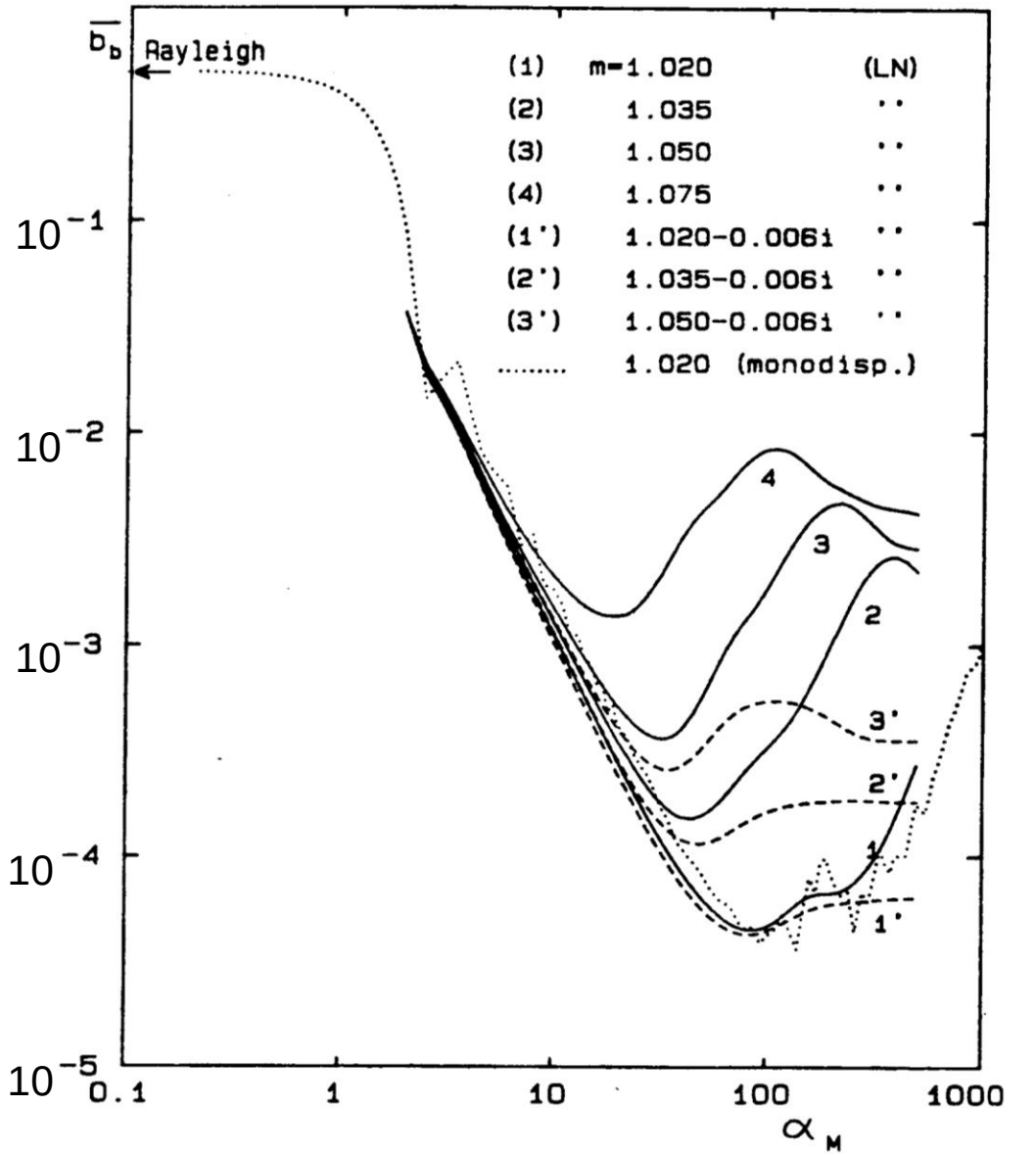

FIG. 8. Variations of the backscattering ratio $\bar{b}_b$ ($= b_b/b$) vs. the modal relative size α_M (same log-normal law as before in Fig. 5). The different curves correspond to various values of the refractive index given in inset. The curve for a monodispersed population (with $m = 1.02$) is also shown (dotted line). The arrow indicates the limiting value of b_b/b ($=0.5$) when α tends toward 0 (Rayleigh domain).

(Morel and Bricaud 1986)

Randomly polarized (unpolarized) light is a jumble of random, rapidly changing **E**-fields

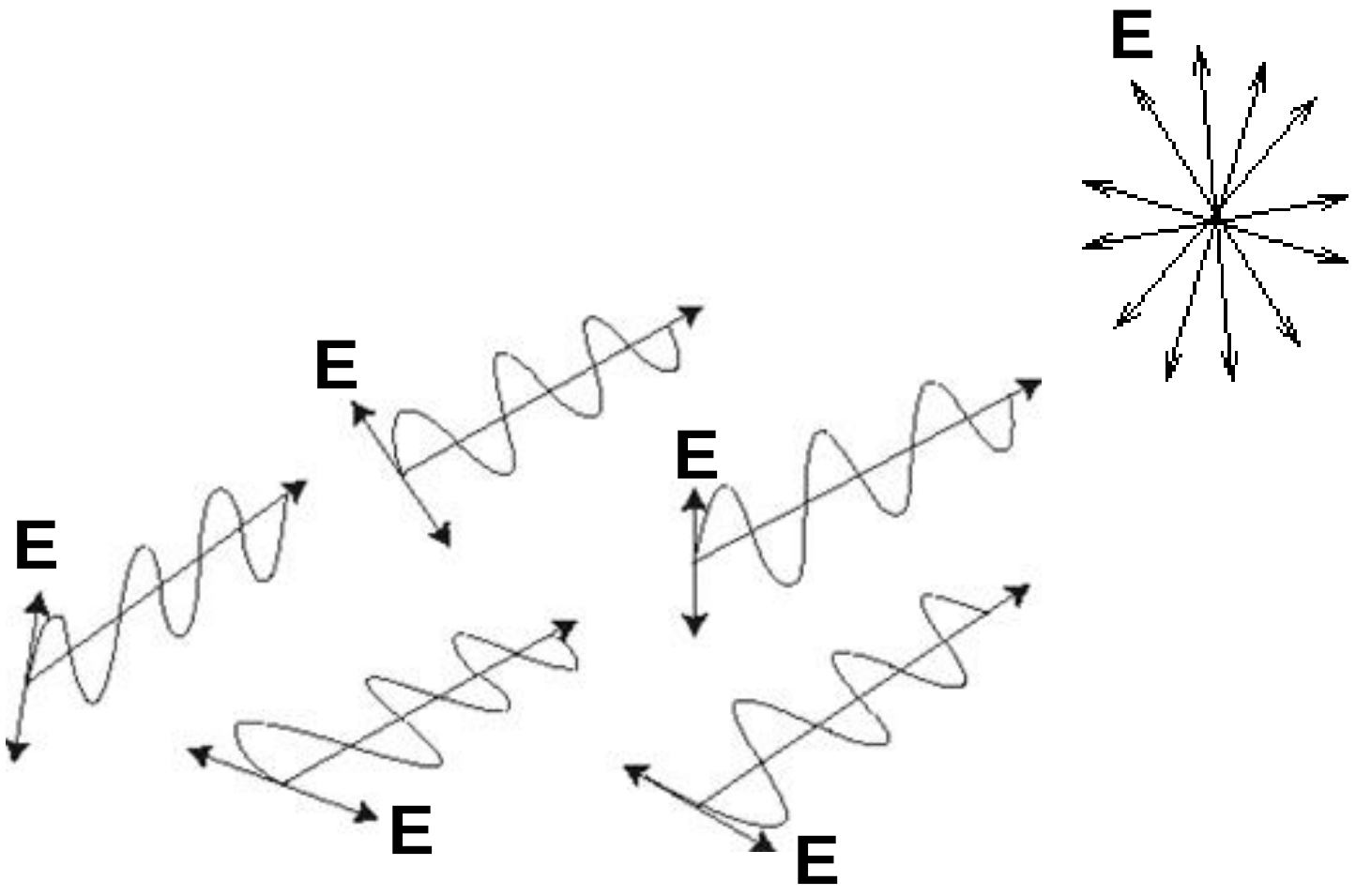

Polarization by scattering

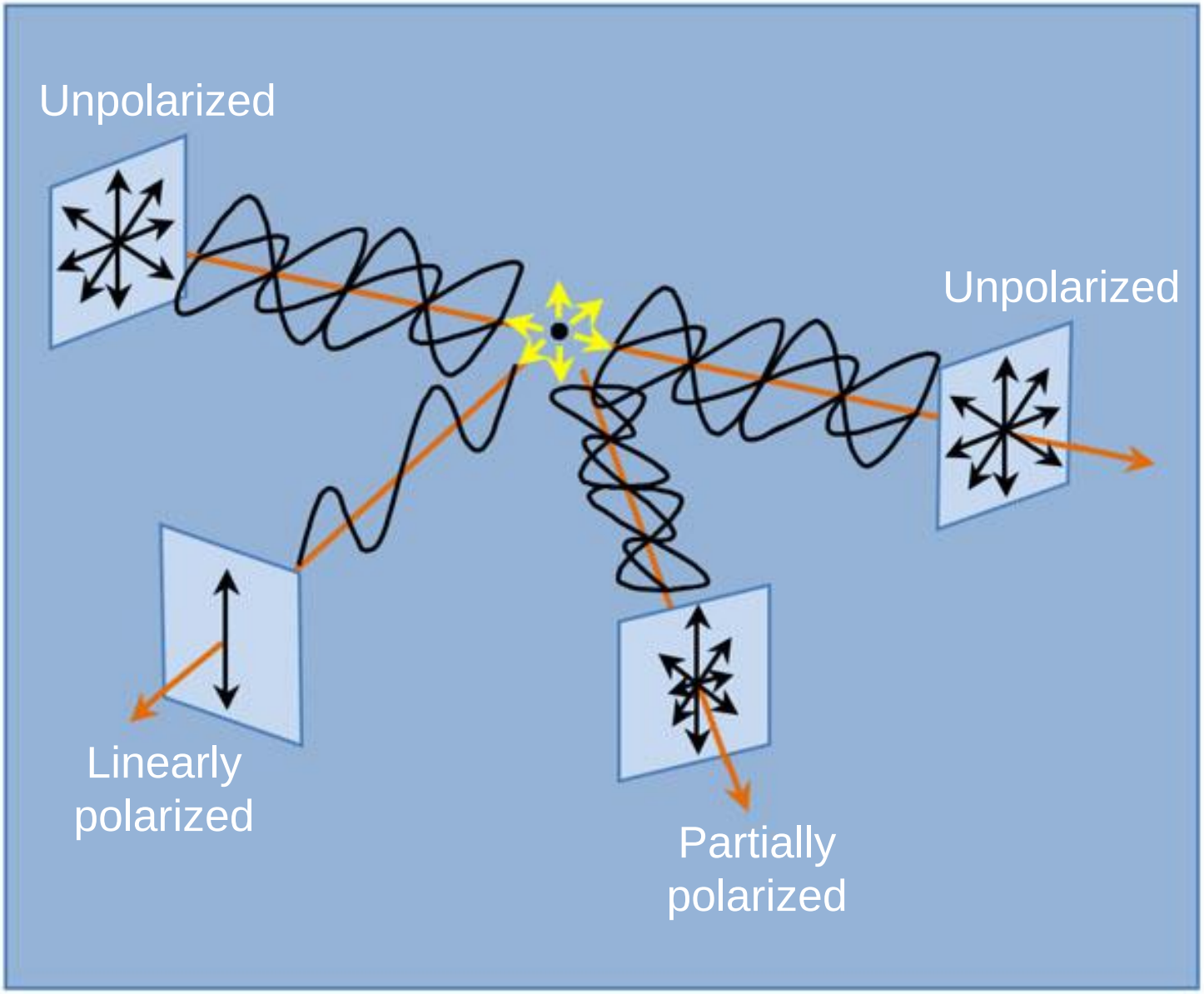

Scattering budget in terms of particle size fractions

Low-index particles

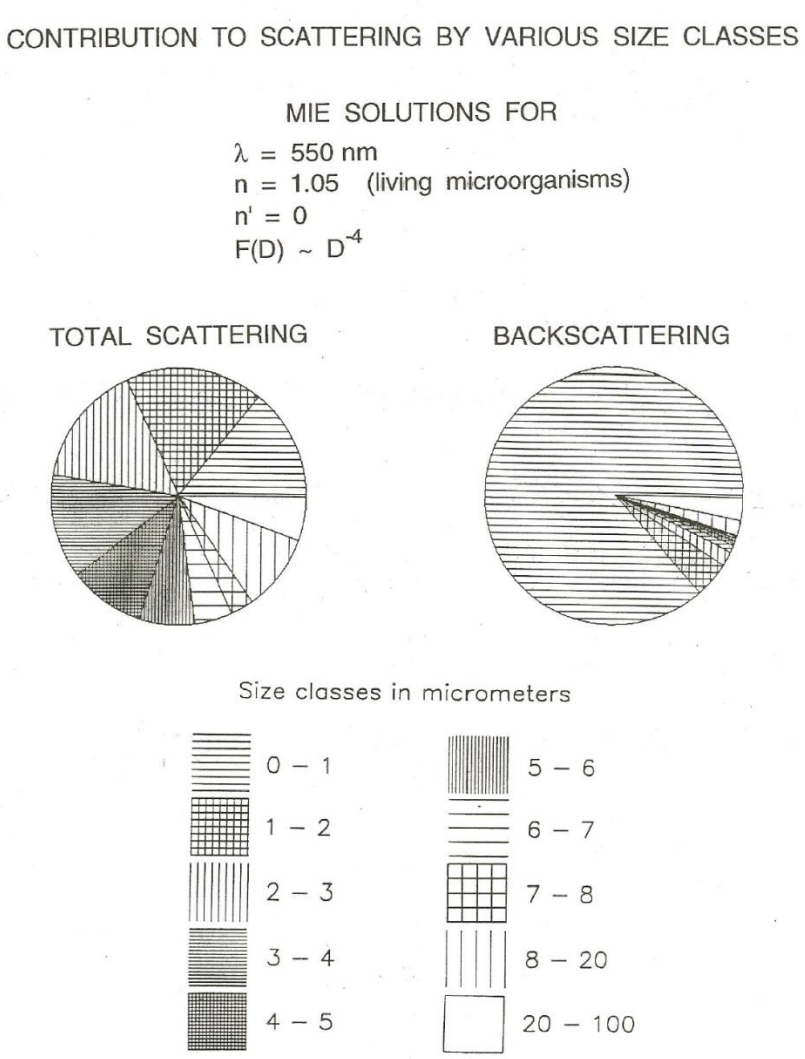

High-index particles

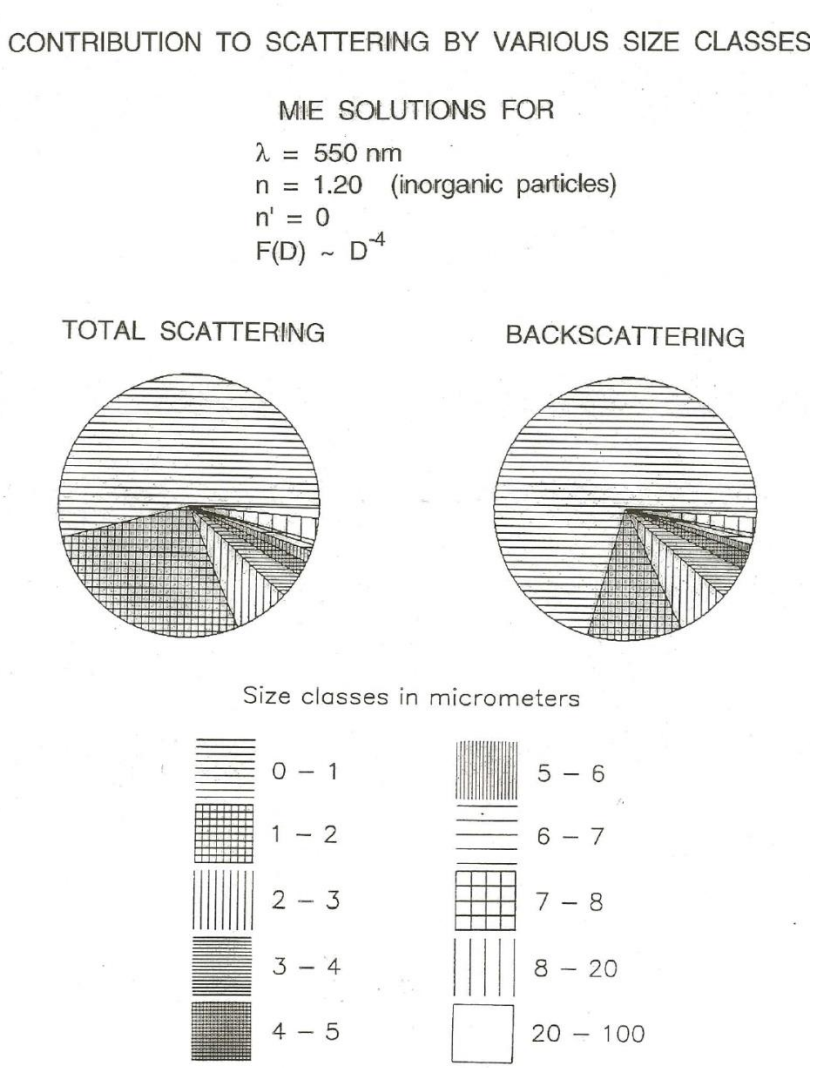

(Stramski and Kiefer 1991)

Particle size from light scattering

Laser diffraction particle sizing technique

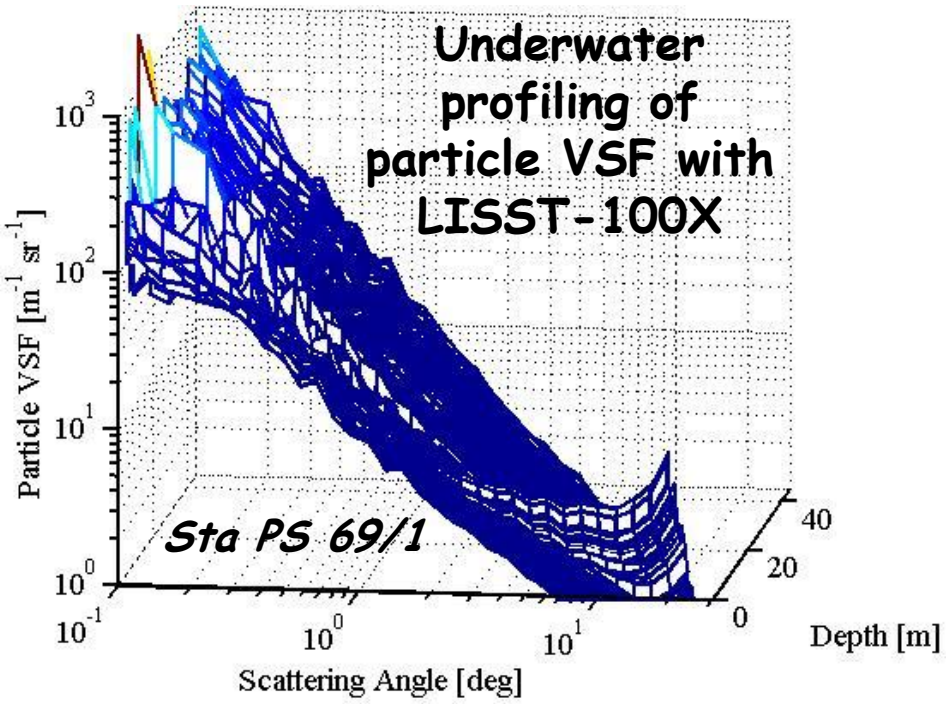

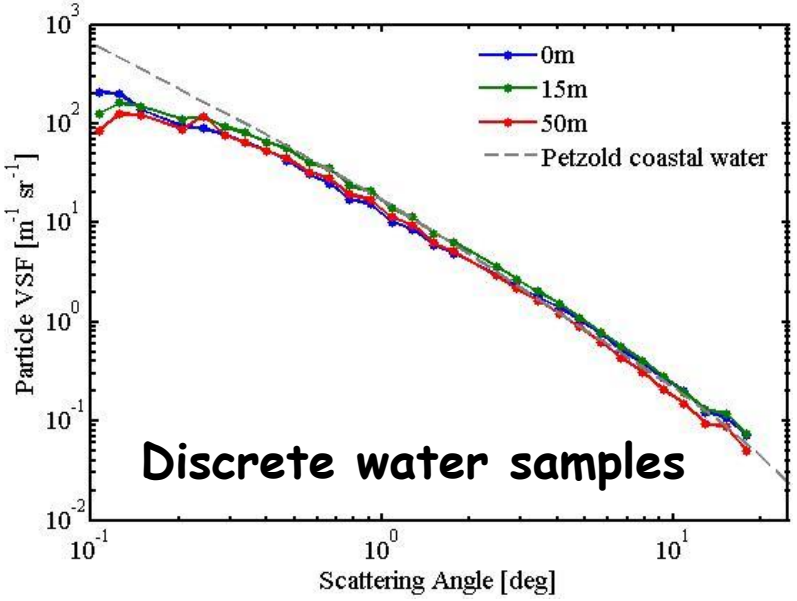

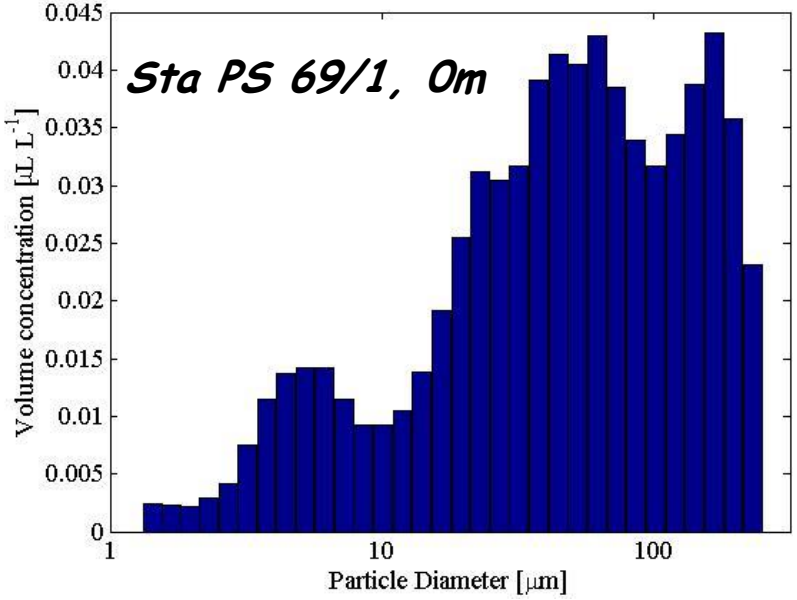

Particle size distribution estimated from Volume Scattering Function (VSF)

(Unpublished data from the Atlantic Ocean)

Cellular carbon and chlorophyll-a from refractive index

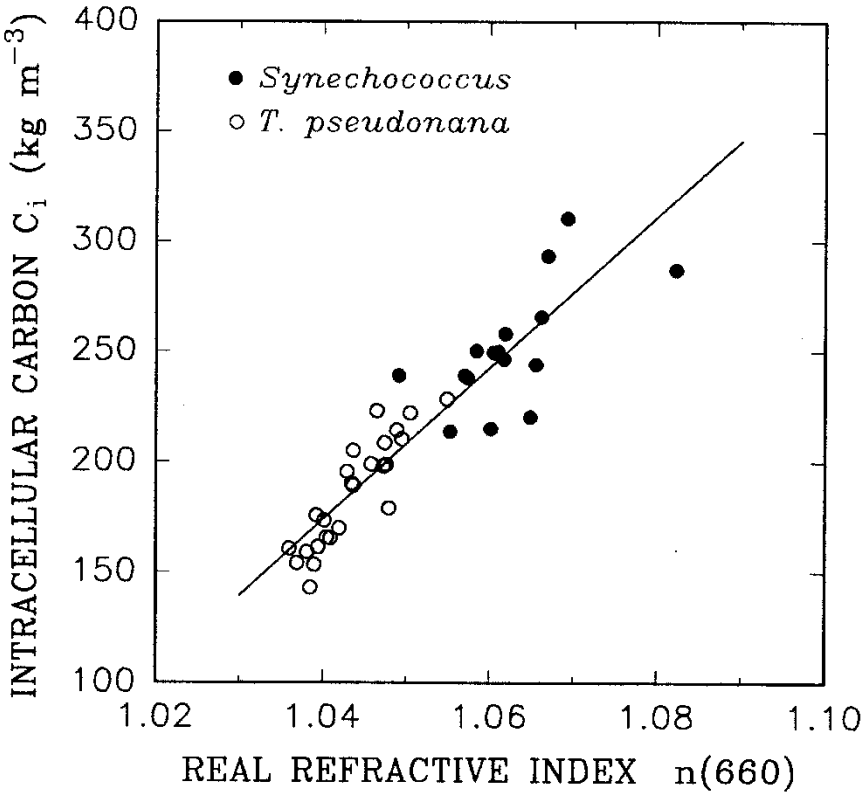

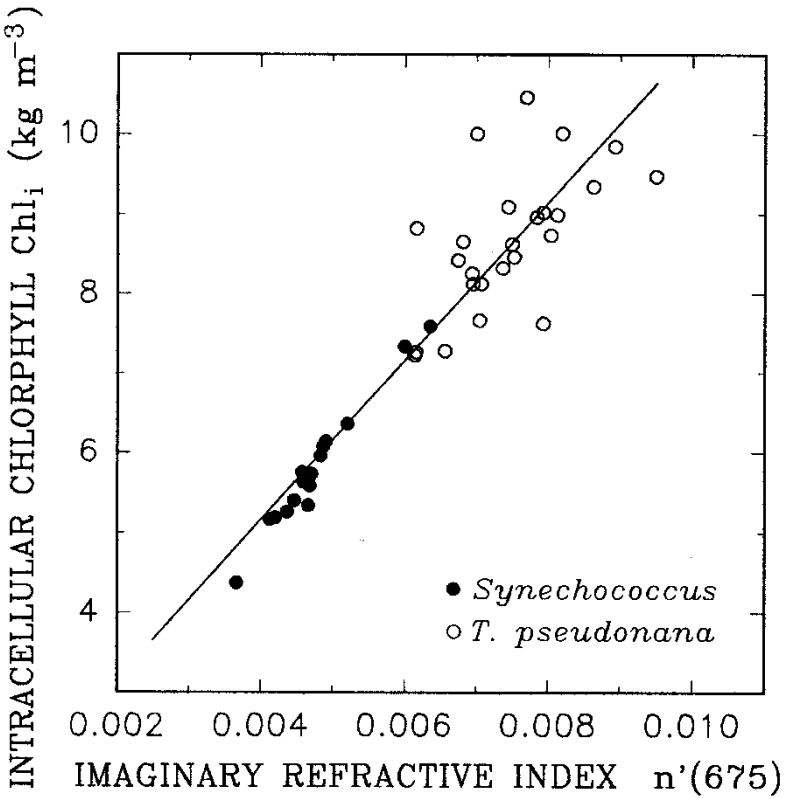

(Stramski 1999)

Cellular carbon and chlorophyll from refractive index

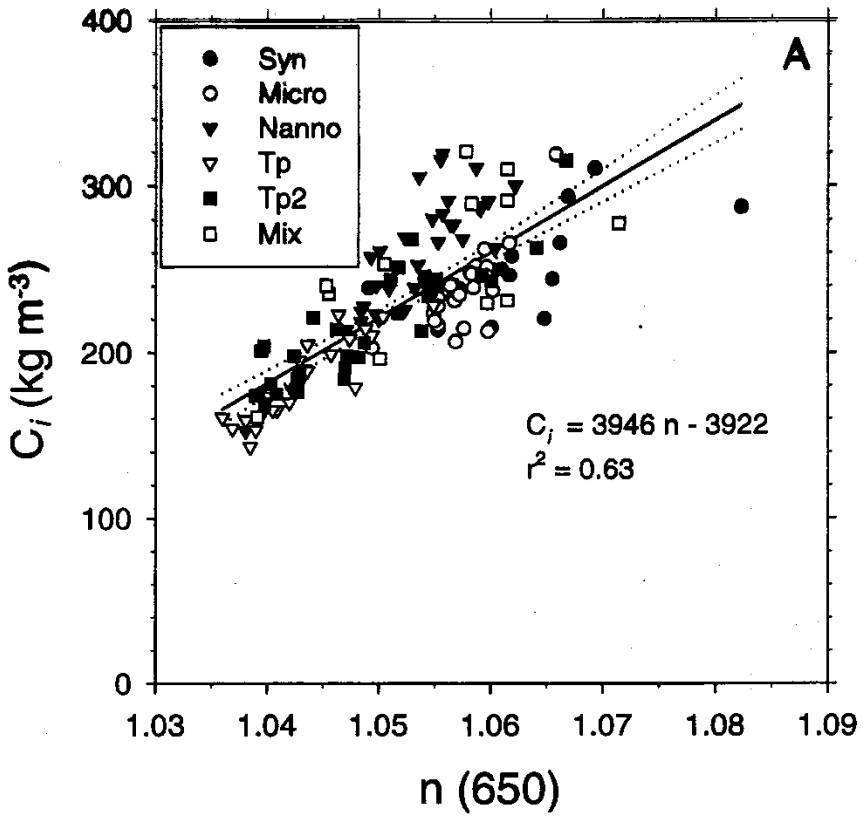

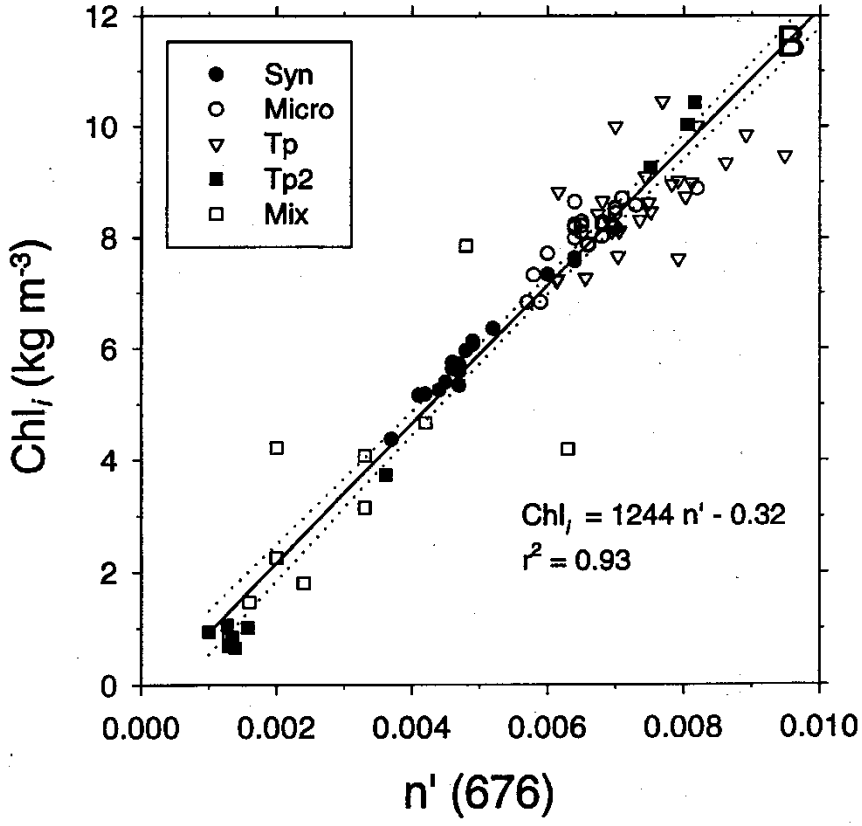

DuRand et al. (2002)

Light scattering on turbulence

• The distribution of light intensity in a Gaussian light beam

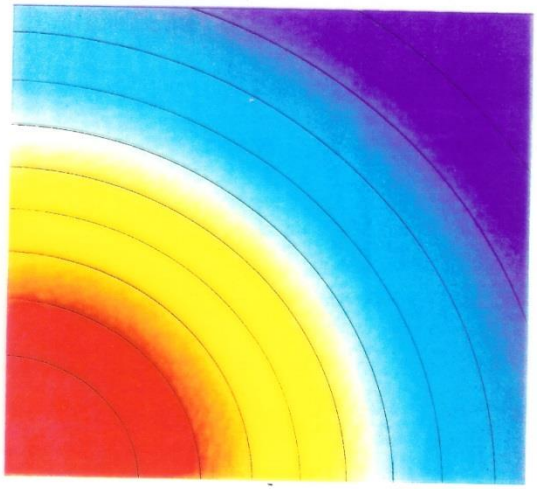

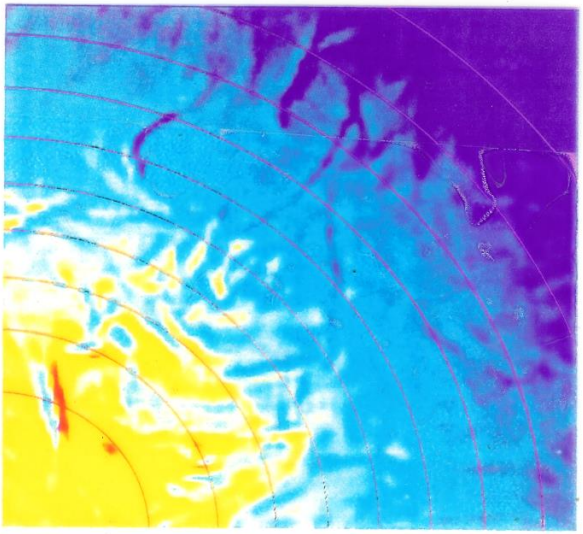

• The actual distribution of light intensity after propagating the distance of 20 cm within a water volume with turbulence looks like this.

(Courtesy of D. Boqucki)

Refractive index n for the extreme values of pressure p, temperature T, salinity S, and wavelength λ, encountered in ocean optics

p (Pa)	T (°C)	S (‰)	λ (nm)	n
1.01×10^5	0	0	400	1.344186
1.01	0	0	700	1.331084
1.01	0	35	400	1.351415
1.01	0	35	700	1.337906
1.01	30	0	400	1.342081
1.01	30	0	700	1.329128
1.01	30	35	400	1.348752
1.01	30	35	700	1.335316
1.08×10^8	0	0	400	1.360076
1.08	0	0	700	1.346604
1.08	0	35	400	1.366885
1.08	0	35	700	1.352956
1.08	30	0	400	1.356281
1.08	30	0	700	1.342958
1.08	30	35	400	1.362842
1.08	30	35	700	1.348986

(Mobley 1994)